Chapter IV - Geochronology and nature of the Palaeoproterozoic basement in the Central African Copperbelt (Zambia and the Democratic Republic of Congo), with regional implications[1]

C. Rainaud[1], S. Master[1], R. A. Armstrong[2], L. J. Robb[1]

[1]Economic Geology Research Institute/ Hugh Allsopp Laboratory, School of Geosciences, University of the Witwatersrand, P. Bag 3, WITS 2050, Johannesburg, South Africa.
[2]PRISE, Research School of Earth Sciences, The Australian National University, Canberra, ACT 0200, Australia

Abstract: U-Pb SHRIMP zircon age data, together with geochemical analyses, from the basement to the Katanga Supergroup in the Central African Copperbelt reveal the existence of a widespread Palaeoproterozoic magmatic arc terrane. The Lufubu schists represent a long-lived calc-alkaline volcanic arc sequence and, where dated in both Zambia and the Democratic Republic of Congo (DRC), yield ages of 1980 ± 7, 1968 ± 9, 1964 ± 12 and 1874 ± 8 Ma. The oldest dated unit from the region, the Mkushi granitic gneiss from south-east of the Zambian Copperbelt, has an age of 2049 ± 6 Ma. The copper-mineralized Mtuga aplites, which crosscut the foliation in the Mkushi gneisses, have mainly xenocrystic, zoned zircons with cores dated at ca. 2.07-2.00 Ga. Overgrowths on these cores are dated at 1059 ± 26 Ma, which is interpreted as the intrusive age of the aplites. An augen gneiss from the Mulungushi Bridge locality yielded an emplacement age of 1976 ± 5 Ma. The Mufulira Pink Granite has an age of 1994 ± 7 Ma, while the Chambishi granite has been dated at 1983 ± 5 Ma, an age within error of Lufubu schist metavolcanics from elsewhere in the Chambishi basin. The gneisses,

[1] *This paper will appear in Special Issue Journal of African Earth Sciences, (Eds.) Robb, Cailteux, Sutton , in press.*

granitoids and acid-intermediate calc-alkaline metavolcanics are considered to represent stages in the evolution of one or more magmatic arcs that formed episodically over a 200 million year period between 2050 and 1850 Ma. We suggest naming this assemblage of rocks the “Lufubu Metamorphic Complex”. The rocks of the Lufubu Metamorphic Complex are interpreted to be part of a regionally extensive Palaeoproterozoic magmatic arc terrane stretching from northern Namibia to northern Zambia and the DRC. This terrane is termed the Kamanjab-Bangweulu arc and is inferred to have collided with the Archaean Tanzanian craton during the ca. 2.0-1.9 Ga Ubendian orogeny, to produce a new composite minicontinental entity that we term the “Kambantan” terrane. The Kambantan terrane was accreted onto the southern margin of the Congo Craton during the ca. 1.4-1.0 Kibaran orogeny.

1. Introduction

The Central African Copperbelt is a world-class stratabound Cu-Co metallogenic province, hosted by Neoproterozoic metasedimentary rocks of the Katanga Supergroup. It extends from the Zambian Copperbelt to the Congolese Copperbelt in the Katanga Province of the Democratic Republic of Congo (DRC) (Robert, 1956; Mendelsohn, 1961a). Much of the age data relating to the Central African Copperbelt was produced in the period 1960-1980 using Rb-Sr and K-Ar techniques (Cahen et al., 1984). The existing data are generally imprecise and their interpretation controversial. In the mid-1990’s a project was undertaken using ion-microprobe U-Pb single zircon technique to provide more accurate time constraints on the Central African Copperbelt. In this study we present new data related to the basement of the Katangan and discuss their significance in terms of the evolution of the Central African Copperbelt. An accompanying paper (Master et al., 2004) presents additional constraints on the provenance ages of the Katanga Supergroup, while the ages of metamorphic events that have affected the Katangan metasediments are presented in Rainaud et al. (2004).

2. Regional geological setting and previous geochronology

The Katanga Supergroup was deformed during the Neoproterozoic to early Palaeozoic eras into an arcuate fold-thrust belt known as the Lufilian Arc. It unconformably overlies a fertile basement which has long been recognised as also containing widespread copper mineralization (Pienaar, 1961; Wakefield, 1978). To the west, the Lufilian Arc is flanked by the c. 1.4-1.0 Ga Kibaran Belt, which separates it from the Neoarchaean and Palaeoproterozoic rocks of the Kasai-Angola Block, which forms part of the larger Congo Craton (Cahen et al. 1984; Delhal, 1991; Tack et al., 1999). To the southeast, the Lufilian Arc is flanked by the Mesoproterozoic Irumide belt (Daly et al., 1984).

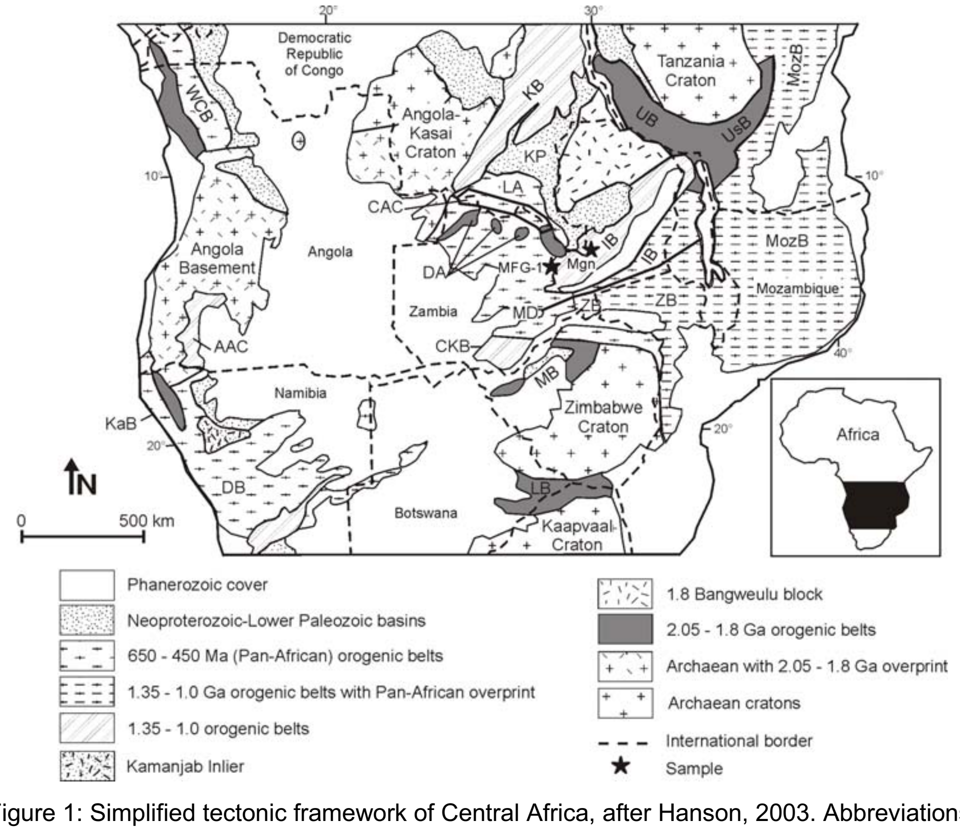

Figure 1: Simplified tectonic framework of Central Africa, after Hanson, 2003. Abbreviations: AAC – Angola Arnothosite Complex; CAC – Central African Copperbelt; DA – Domes area; DB – Damara belt; IB – Irumide belt; KaB – Kaoko belt; KB – Kibaran belt; CKB – Choma-Kalomo block; KP – Kundelungu Plateau; LA – Lufilian arc; LB – Limpopo belt; MB – Magondi belt; MD – Mwembeshi dislocation; MozB – Mozambique belt; UB – Ubendian belt; UsB – Usagaran belt.

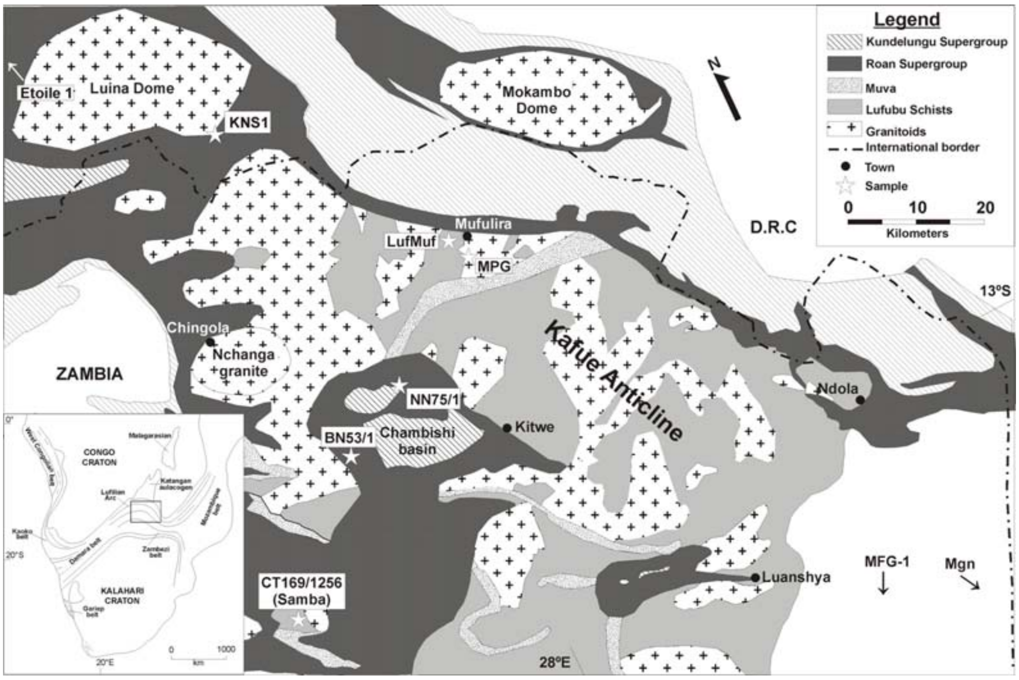

Figure 2: Simplified geological map of the eastern Copperbelt and location of samples after François, 1984.

Although the Central African Copperbelt extends through both the Democratic Republic of Congo and Zambia and has a strike length of 700 km in the Lufilian Arc (Figure 1 and 2), the pre-Katangan basement is mainly exposed in Zambia and immediately adjacent areas of the Democratic Republic of Congo (Brock, 1961; Demesmaeker et al., 1963). This fact, and other lithological and structural factors, led François (1974) to distinguish two provinces in the Central African Copperbelt: the Zambian Province, extending from Zambia to the Congolese deposits close to the border (such as Musoshi and Kinsenda), and the Congolese Province, extending from Lubumbashi to Kolwezi. In the Zambian Province, the basement rocks are exposed in a structural high known as the Kafue Anticline (Garlick, 1961a). In adjacent areas of Katanga, basement exposures are found in the Konkola, Luina and Mokambo Domes (Gysin, 1933; Lecompte, 1933). About half of the pre-Katangan basement consists of the Lufubu schists, and the rest consists mainly of a variety of supposedly intrusive granitoids (Gray, 1929; Mendelsohn, 1961b,c). Some of these granitoids were previously regarded as also being intrusive into the Katangan sequence, but this was disproven by Garlick and Brummer (1951), who showed that all granites in the Copperbelt are of pre-Katangan age, and are unconformably overlain by Katangan rocks. Post-Katangan intrusive granitoids form several plutons in the western and southern exposed parts of the Lufilian arc in Zambia (Thieme and Johnson, 1981) and in the Hook massif and adjacent areas of the inner part of the Lufilian arc (Hanson et al., 1993). The granitoids intrusive into the Lufubu schists were first dated by Cahen et al. (1968, 1970b,c) using bulk zircon U-Pb dating, and were shown to represent a Palaeoproterozoic magmatic suite with imprecise ages spanning 2018-1702 Ma (Cahen et al., 1984). Cahen et al. (1970c) dated the Grey Granodiorite at Mufulira using two near-concordant bulk zircon fractions. Depending on whether Pb-loss was assumed to be at zero age (model 1), or whether it occurred during the Kibaran orogeny at c. 1300 Ma (model 2), they obtained model ages of 1945 Ma (model 1) to 2018 Ma (model 2) for the Mufulira Grey Granodiorite (Cahen et al., 1984). The Roan Antelope Granite at Luanshya yielded a (recalculated) $^{207}Pb/^{206}Pb$ isochron age, based on four bulk zircon fractions, of 1702 Ma (Cahen et al., 1970c; 1984). Cliff and Clemmey (1976) obtained a Rb-Sr model age of ca. 2 Ga on muscovite from a pegmatite cutting basement rocks at Mindola Mine. A granitoid from the Luina Dome in the DRC, close to the Zambian Copperbelt, has been dated at 1882 +23/-19 Ma (Ngoyi et al., 1991). The Lufubu schists were constrained to be older than 2049 ± 103 Ma to 2198 ± 108, based on a model Rb-Sr age of a post-Lufubu, pre-Katangan pegmatite, with assumed initial $^{87}Sr/^{86}Sr$ ratios in the range 0.705 to 0.710 (Cahen et al., 1970a, 1984).

The Palaeoproterozoic basement rocks of the Copperbelt extend northwards to the Luapula Province of Zambia and the Marungu Plateau of the DRC, southwest of Lake Tanganyika, where they constitute the basement of the Bangweulu Block (Drysdall et al., 1972; Brewer et al., 1979; Kabengele et al., 1990; Andersen and Unrug, 1984). Brewer et al. (1979) obtained Rb-Sr isochron ages of 1816 ± 22 Ma and 1833 ± 18 Ma, for a rhyolite and a granitoid from the western part of the Bangweulu Block. These rocks have relatively low initial $^{86}Sr/^{86}Sr$ ratios (R_i) of 0.70328 and 0.70327, respectively, indicating a similar source in the juvenile crust or upper mantle. In the Marungu Plateau, three intrusive complexes have yielded whole-rock Rb-Sr isochron ages of 1863 ± 53 Ma, 1861 ± 28 Ma and 1695 ± 43 Ma, with R_i = 0.70277, 0.7026 and 0.70436 respectively (Kabengele et al., 1990). In northeast Zambia, granitoids of the Bangweulu Block have yielded whole-rock Rb-Sr isochron ages of 1869 ± 20 Ma, 1838 ± 43 Ma and 1824 ± 75 Ma (Schandelmeier, 1981, 1983).

To the southeast of the Copperbelt, the Irumide Belt of northeast Zambia consists of quartzites and metapelites of the Manshya River Group, together with syntectonic to late-tectonic granitoid plutons, amphibolite-facies gneisses, and migmatites (Daly, 1986; Tembo et al., 2002; de Waele and Mapani, 2002). A metarhyolite interbedded with metasediments from the northern part of the belt in the Chinsali area has yielded a SHRIMP U-Pb zircon age of 1880 ± 12 Ma, which gives the depositional age for the Manshya River Group (de Waele and Mapani, 2002). Syn- to late-tectonic intrusive granitoids in the Irumide belt are dated at between 1046 ± 77 Ma and 953 ± 19 Ma, with a metamorphic peak at ca. 1020 Ma (de Waele et al., 2003; SHRIMP U-Pb single zircon dates). Monazite growth at ultrahigh-temperature peak metamorphic conditions (T = 875°-900°C; P ~ 6 kb) took place at 1046 ± 3 Ma in garnet-cordierite gneisses in the eastern Irumide Belt near Chipata (Schenk and Appel, 2001, 2002). The basement to the Irumide Belt consists partly of granitoid gneisses referred to as the Mkushi Gneisses. These are intruded by the Mtuga granites and associated aplites (which are mineralized with Cu at the Mkushi Mine; Legg, 1976). The Mkushi Gneisses yielded a whole-rock Rb-Sr date of 1777 ± 89 Ma, while the Mtuga granite yielded a date of 607 ± 39 Ma (N'gambi et al., 1986). A model Rb-Sr age of 1693 ± 50 Ma (assuming R_i = 0.709) was obtained for an aplite from Mkushi (Cahen and Snelling, 1966; recalculated by Cahen et al., 1984). Recent SHRIMP zircon dating by de Waele et al. (2003) of the Lukamfwa Hill granitic gneisses, between Mkushi and Serenje in the western part of the central Irumide Belt, yielded ages between 1664 ± 9 Ma and 1639 ± 14 Ma. Other gneissic granites from the northern Irumide Belt have yielded zircon ages of 1592 ± 43 Ma and 1519 ± 19 Ma (de Waele et al., 2003).

In the Copperbelt region, the Lufubu schists and the intrusive granitoids are unconformably overlain by quartzites and schists of the Muva Supergroup (Garlick, 1961b). The Muva metasediments have a maximum age of 1941 ± 40 Ma, which is the age of the youngest detrital zircon dated by Rainaud et al. (2003) from these sediments. The youngest pre-Katangan intrusive in the basement is the Nchanga Granite, with a SHRIMP zircon age of 877 ± 10 Ma, which gives the maximum age for Katangan sedimentation (Armstrong et al., 1999, 2004).

3. Analytical methods

Major element analyses were performed using X-Ray Fluorescence Spectrometry on a Philips spectrometer, in the Department of Geology, School of Geosciences, University of the Witwatersrand. Major elements were determined using the fusion technique of Norrish and Hutton (1969). Trace element analyses were done on pressed powder pellets by XRF using the method of Feather and Willis (1976).

The separation of zircons was carried out at the Hugh Allsopp Laboratory, Johannesburg, using conventional techniques. The separated zircons were examined and characterised in term of uranium contents using the cathodoluminescence technique. All zircons were randomly selected for analysis, but the locations of the analysed spots were chosen to avoid areas of anomalously high or low uranium contents. U-Pb analyses were performed on the Sensitive High Resolution Ion Microprobe (SHRIMP) I and II at the Australian National University, Canberra. The SHRIMP analytical procedure used in this study is similar to that described by Claoué-Long et al. (1995). Age calculations and plotting of analytical data were carried out using Isoplot/Ex (Ludwig, 2000) and all ages are quoted with errors at the 1σ level.

4. Results

A total of eleven samples were dated for the purposes of this study, representing Lufubu schist metavolcanics (4 samples), and granitoids and granitoid gneisses (7 samples) from the basement to the Katanga Supergroup of the Central African Copperbelt and from an adjacent area in the Irumide Belt. Nine of these samples were collected in Zambia and two in the Democratic Republic of Congo (Figure 1 and 2).

a. Lufubu schists

Gray (1929) first differentiated highly deformed Lufubu schists and gneisses from overlying Muva metasedimentary rocks. Jackson (1932) called the Lufubu schists of the Nchanga area the “Basement Schist Series”, consisting of garnetiferous chlorite schists, quartz-mica schists and biotite gneisses, which he regarded as being metasedimentary in origin and Archaean in age. Mendelsohn (1961b) described the Lufubu schists as mica schists, quartzites and gneisses with minor metamorphosed carbonates, conglomerates, subgraywackes and arkoses, extensively intruded by granites. He regarded the majority of the Lufubu schists as metasediments with the possibility of some minor metavolcanics. Unconformably overlying the Lufubu schists are the Muva metasediments, which consist of deformed quartzites, metaconglomerates and metapelitic schists (Garlick, 1961b).

Geochemistry of the Lufubu schists

Whole-rock geochemistry was undertaken on Lufubu schists from the Mwambashi B prospect in the Chambishi basin, Baluba Mine near Luanshya, the Kafue River south of Mufulira (Figure 3) and from Kinsenda in the DRC. Samples were analysed for both major and trace elements (Table 1), and were examined petrographically for their mineralogical and textural characteristics. All samples present porphyritic textures with fine grained-matrices of metamorphic sericite. Lufubu schist compositions are presented in a Zr/TiO_2 vs Nb/Y diagram (Winchester and Floyd, 1977) (Figure 4) which shows that these rocks plot in the andesite/ rhyodacite-dacite/ trachyandesite/ alkali basalt domain. The sample suite has characteristics consistent with a metavolcanic origin. The same analyses together with those from the host rocks of the Samba porphyry (Wakefield, 1978) are plotted in the AFM geochemical discrimination diagram of Irvine and Baragar (1971) (Figure 5). All analyses show enrichments in the alkalis Na_2O+K_2O compared to FeO, and they plot in the calc-alkaline field. Because these rocks may have suffered mobility of major elements during metamorphism, the AFM plot can only be used to suggest that the data are consistent with the Lufubu schists being mainly calc-alkaline metavolcanic rocks. The Lufubu schist metavolcanic rocks, together with subordinate metasedimentary rocks such as quartzites and marbles, are regarded as having formed in a subduction-related magmatic arc.

Figure 3: Lufubu schists in the Kafue River south of Mufulira showing multiple cleavages and polyphased deformation involving the folding of an earlier fabric

Table 1: Trace and major element analyses of the Lufubu schists

	Baluba							Kinsenda	Kafue River		Chambishi
Samples	**Ba1**	**Ba2**	**Ba3**	**Ba4**	**Ba5**	**Ba6**	**Ba7**	**KNS1**	**L1**	**L2**	**BN53/1**
SiO2	73.29	73.41	72.38	61.99	62.33	65.66	72.77	58.74	55.59	67.80	60.22
TiO2	0.21	0.22	0.17	0.68	0.70	0.65	0.49	0.97	0.94	0.88	0.58
Al2O3	13.72	13.61	14.20	16.75	16.91	15.38	13.84	18.19	19.49	13.12	15.52
Fe2O3	1.43	1.59	1.82	5.10	5.23	2.22	3.39	5.90	9.35	8.08	7.00
MnO	0.04	0.05	0.05	0.04	0.02	0.03	0.01	0.11	0.17	0.17	0.12
MgO	0.59	0.64	0.96	3.32	3.42	3.63	2.23	4.04	3.26	3.13	4.17
CaO	2.14	1.62	1.66	0.94	0.70	1.86	0.29	0.54	2.35	1.27	0.98
Na2O	4.59	4.57	5.71	8.14	8.04	7.83	0.40	3.19	3.12	2.25	0.90
K2O	2.63	2.88	2.05	2.16	2.14	1.24	4.88	7.74	2.67	2.24	6.18
P2O5	0.05	0.05	0.07	0.10	0.08	0.06	0.14	0.30	0.20	0.12	0.13
LOI	1.73	1.50	1.80	1.31	1.21	1.88	2.15	1.48	2.69	1.83	3.18
Total	100.41	100.14	100.88	100.53	10.76	100.45	100.65	101.20	100.32	100.89	98.98
Rb	64	65	67	59	59	44	152	272	236	209	236
Sr	121	114	129	85	87	223	42	103	233	154	40
Y	30	35	52	20	18	7	8	37	41	42	18
Zr	99	105	44	149	150	171	80	336	219	266	111
Nb	21	23	23	11	10	10	12	33	19	15	13
Co	12	11	14	26	23	14	31	20	27	23	298
Ni	9	9	10	72	68	97	29	13	90	69	41
Cu	2	2	38	25	10	2	2	29	47	8	<9
Zn	10	11	17	35	30	55	17	96	95	73	82
V	15	15	22	130	126	79	133	86	103	74	107
Cr	13	11	12	221	220	208	93	21	161	135	45
Ba	588	602	448	770	797	217	1335	1760	458	383	1343

Table 1: Trace and major element analyses of the Lufubu schists
Samba (Wakefield, 1978)

Samples	MN149	MN150	MN152	MN153	MN154
SiO2	70.32	70.76	67.70	65.06	66.21
TiO2	0.61	0.71	0.57	0.59	0.55
Al2O3	14.00	14.54	15.41	16.31	15.01
Fe2O3	2.21	3.50	2.08	1.86	2.09
MnO	0.08	0.05	0.11	0.10	0.13
MgO	1.31	0.96	2.05	2.17	1.75
CaO	2.58	1.70	1.38	1.90	2.75
Na2O	2.32	2.90	2.38	3.56	3.62
K2O	3.12	3.20	3.41	3.19	3.09
P2O5	0.13	0.12	0.10	0.12	0.10
LOI	-	-	-	-	-
Total	99.97	100.88	100.10	99.37	99.73

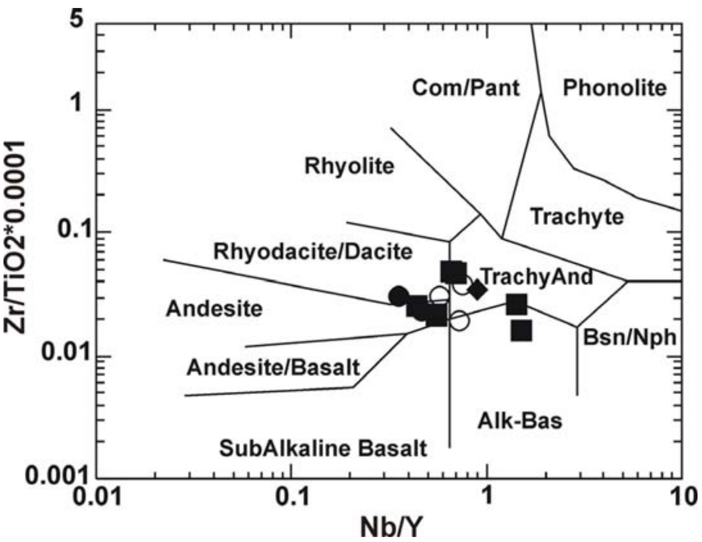

Figure 4: Zr/TiO_2 vs Nb/Y geochemical classification diagram (Winchester and Floyd, 1977) for the Lufubu schists. Filled squares – Lufubu schists from Mufulira; filled circles – Lufubu schists from Kafue River, south of Mufulira; diamond – Lufubu schists from Kinsenda; empty square – BN53/1 from the Mwambashi B prospect in the Chambishi basin.

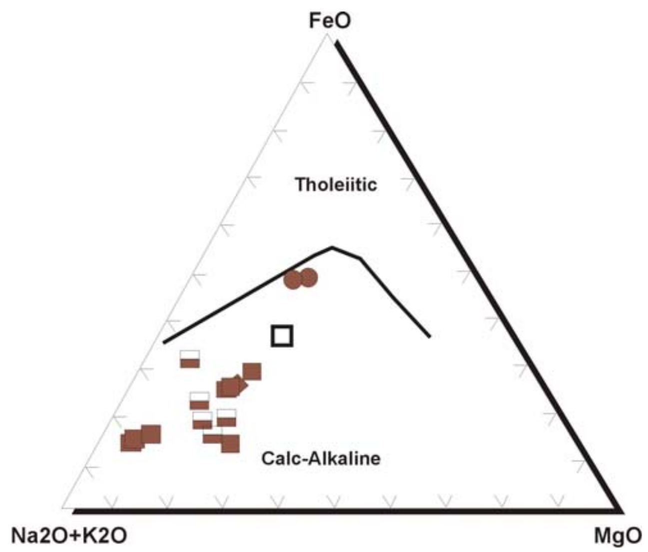

Figure 5: AFM diagram (Irvine and Baragar, 1971) of the Lufubu schists. Filled squares – Lufubu schists from Mufulira; filled circles – Lufubu schists from Kafue River, south of Mufulira; diamond – Lufubu schists from Kinsenda; empty square – BN53/1 from the Mwambashi B prospect in the Chambishi basin; half filled squares – host rocks of the Samba porphyry Cu deposit.

Mufulira Lufubu schist (sample LufMuf)

Sample LufMuf was collected from the Mufulira Mine, on the eastern flank of the Kafue anticline (Figure 2). It is a blastoporphyritic metavolcanic derived from a hornblende-quartz porphyry in which the fine-grained matrix and amphibole-phenocrysts are replaced by intergrowths of epidote, biotite, chlorite, quartz magnetite and sphene (Figure 6).

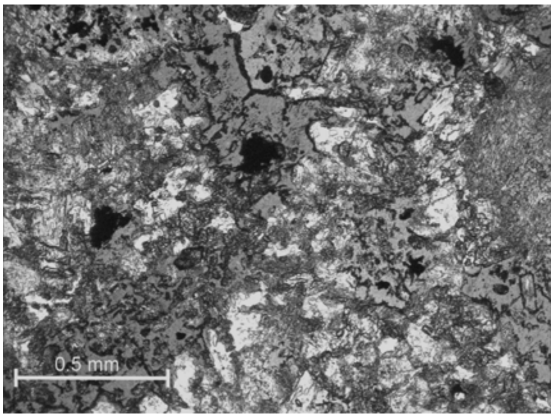

Figure 6: Photomicrograph of the Mufulira Lufubu schist, sample LufMuf.

Fourteen analyses were undertaken on 14 zircons from this sample. Cathodoluminescence images and plane-polarised photomicrographs (Figure 7) show three types of zircons; euhedral, broken and abraded. All zircons exhibit an oscillatory zoning consistent with an igneous origin. The c-axes of the zircons are up to 200 μm in length. Euhedral zircons represent more than 50% of the entire population.

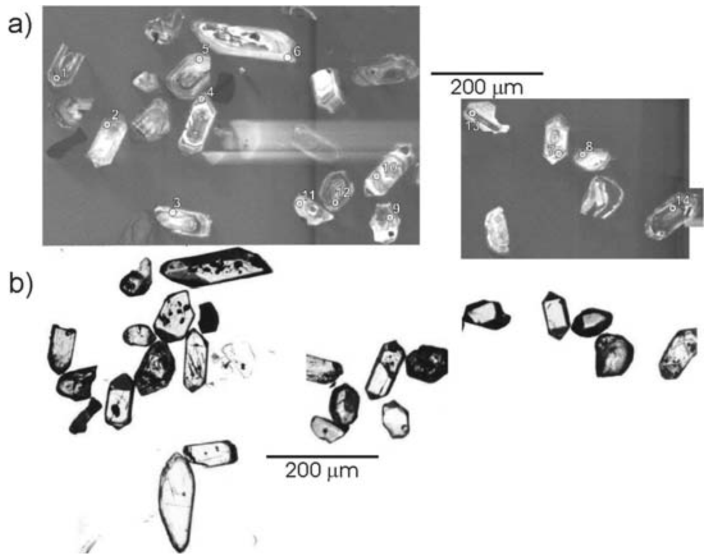

Figure 7: Sample LufMuf a) Cathodoluminescence image of the analysed zircons. White circles show location of analyses; b) Photomicrograph of the zircons.

Results of the analyses are reported in Table 2 and plotted on a concordia diagram in Figure 8. Two distinct populations and one older single zircon (zircon no. 8 on the CL image and in Table 2) are evident. The oldest zircon yields a $^{207}Pb/^{206}Pb$ age of 2174 ± 13 Ma. The older of the two main populations includes three zircons (zircons no. 1, 5 and 11), all broken pieces, which yield a weighted mean $^{207}Pb/^{206}Pb$ age of 2057 ± 9 Ma (MSWD = 1.8). It is unclear whether these zircons were broken during their incorporation as xenocrysts, or if they were broken during sample preparation. The youngest population consists of ten zircons (zircons no. 2, 3, 4, 6, 7, 9, 10, 12, 13 and 14 on the CL image and in Table 2) and yielded an average mean $^{207}Pb/^{206}Pb$ age of 1968.1 ± 9.3 Ma with a MSWD = 1.6. On the CL image, these ten zircons are euhedral. An attempt at differentiating the three populations of zircons by plotting age versus Th/U ratio was made (Figure 9). Th/U results from the youngest population (mean age at 1968.1 ± 9.3 Ma) are scattered and vary between 0.36 and 2.18. The group of three broken zircons plots between 0.63 and 0.88. The oldest single zircon has the lowest Th/U ratio of 0.34. Thus, there appears to be an inverse exponential trend between Age and Th/U ratios; however, no definitive interpretation can be made, as the data set is not large enough. The age of the youngest population (1968 ± 9 Ma) is interpreted as the age of the protolith of the Lufubu metavolcanics at Mufulira. This interpretation is consistent with the igneous characteristics of the dated grains. The four older zircons are regarded as inherited.

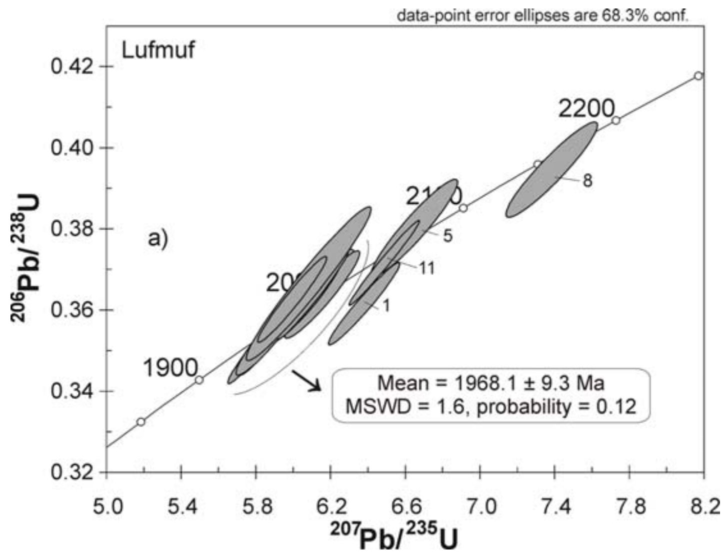

Figure 8: Concordia plot of zircon analyses for the Mufulira Lufubu schist sample (LufMuf).

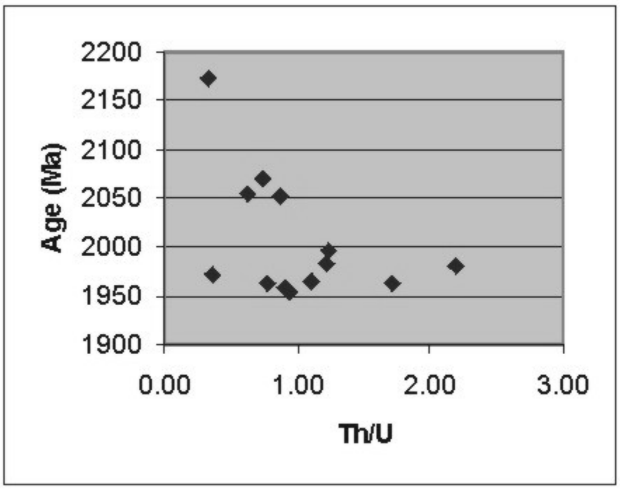

Figure 9: Age vs. Th/U of the analysed zircons for sample LufMuf.

Table 2 . Summary of SHRIMP U-Th-Pb zircon results for sample LUFMUF

							Radiogenic Ratios						Ages (in Ma)						
Grain. spot	U (ppm)	Th (ppm)	Th/U	Pb (ppm)	$^{204}Pb/^{206}Pb$	f_{206} %	$^{206}Pb/^{238}U$	±	$^{207}Pb/^{235}U$	±	$^{207}Pb/^{206}Pb$	±	$^{206}Pb/^{238}U$	±	$^{207}Pb/^{235}U$	±	$^{207}Pb/^{206}Pb$	±	Conc. %
1	411	306	0.74	171	0.000066	0.10	0.3614	0.0067	6.378	0.126	0.1280	0.0006	1989	32	2029	17	2071	8	96
2	184	170	0.92	78	0.000042	0.06	0.3532	0.0076	5.845	0.133	0.1200	0.0006	1950	36	1953	20	1957	9	100
3	150	183	1.22	69	0.000047	0.07	0.3640	0.0072	6.114	0.139	0.1218	0.0011	2001	34	1992	20	1983	16	101
4	135	166	1.23	62	0.000094	0.14	0.3637	0.0072	6.153	0.133	0.1227	0.0009	2000	34	1998	19	1996	12	100
5	138	87	0.63	59	0.000102	0.16	0.3803	0.0079	6.649	0.153	0.1268	0.0010	2078	37	2066	21	2054	13	101
6	164	59	0.36	63	0.000084	0.13	0.3624	0.0075	6.049	0.141	0.1211	0.0010	1994	36	1983	21	1972	15	101
7	165	150	0.91	71	0.000059	0.09	0.3612	0.0069	5.985	0.126	0.1202	0.0008	1988	33	1974	18	1959	12	102
8	107	36	0.34	45	0.000032	0.05	0.3947	0.0078	7.386	0.163	0.1357	0.0010	2144	36	2159	20	2174	13	99
9	234	258	1.10	102	0.000043	0.06	0.3537	0.0065	5.884	0.114	0.1207	0.0005	1952	31	1959	17	1966	8	99
10	163	126	0.77	67	0.000081	0.12	0.3541	0.0068	5.877	0.124	0.1204	0.0008	1954	32	1958	19	1962	12	100
11	442	389	0.88	195	0.000043	0.06	0.3715	0.0069	6.486	0.125	0.1266	0.0004	2037	33	2044	17	2052	6	99
12	241	526	2.18	133	0.000009	0.01	0.3637	0.0072	6.102	0.127	0.1217	0.0005	2000	34	1991	18	1981	8	101
13	398	679	1.71	202	0.000149	0.23	0.3664	0.0126	6.081	0.222	0.1204	0.0011	2013	60	1988	32	1962	16	103
14	222	207	0.93	96	0.000035	0.05	0.3625	0.0070	5.991	0.123	0.1199	0.0006	1994	33	1975	18	1954	9	102

Notes :

1. Uncertainties given at the one σ level.
2. f_{206} % denotes the percentage of ^{206}Pb that is common Pb.
3. Correction for common Pb made using the measured $^{204}Pb/^{206}Pb$ ratio.
4. For % Conc., 100% denotes a concordant analysis following Tera and Wasserburg (1972) as outlined in Compston et al. (1991).

Kinsenda meta-trachyandesite (sample KNS1)

Sample KNS1 was collected at Kinsenda Mine (DRC) on the southern flank of the Luina Dome near the border with Zambia (Figure 2 and 10).

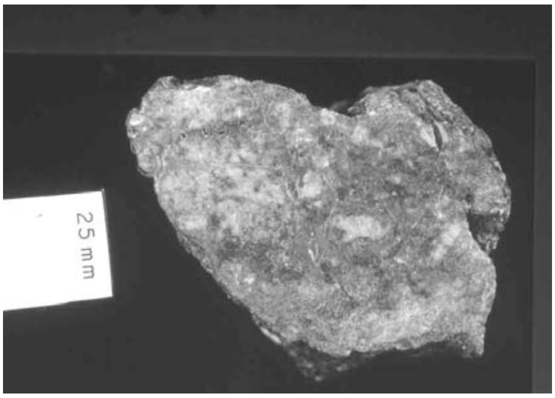

Figure 10: Hand specimen of the Kinsenda Lufubu schist, KNS1.

It is a metatrachyandesitic porphyry with relict alkali-feldspar phenocrysts showing perthitic texture (Figure 11). Feldspar phenocrysts are quite deformed (some are kinked) and the matrix of biotite and muscovite shows two generations of metamorphic muscovite.

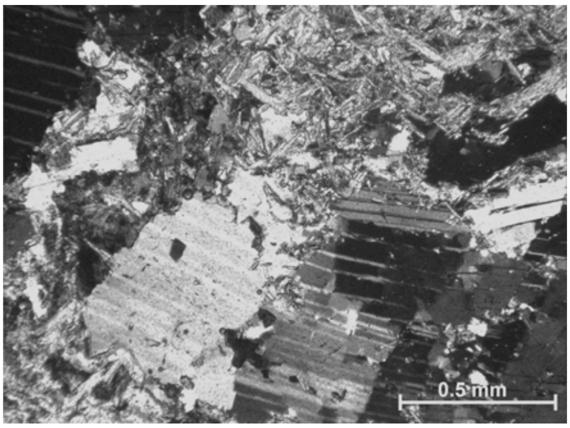

Figure 11: Photomicrograph of the Kinsenda Lufubu schist (KNS1).

Cathodoluminescence imaging shows that the zircons are large (Figure 12), with the long axis ≥ 200 μm. All zircons exhibit an oscillatory zoning consistent an igneous origin. Sixteen analyses were undertaken on 15 zircons (Table 3, Figure 13). All analyses are concordant or less than 15%

discordant and plot in a single cluster. All the analyses yielded a weighted mean $^{207}Pb/^{206}Pb$ age of 1873.5 ± 8.3 Ma (MSWD = 1.7). This age is interpreted as the igneous age of the trachyandesitic protolith of the Lufubu schist at Kinsenda.

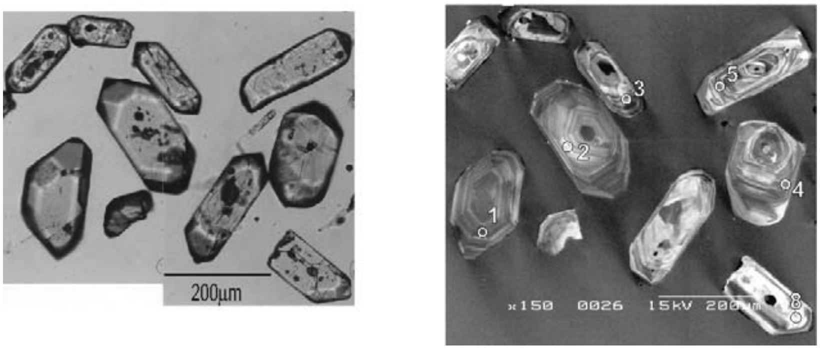

Figure 12: Photomicrograph and cathodoluminescence images of some of the analysed zircons from the Kinsenda Lufubu schist, sample KNS1. White circles represent the points of analyses.

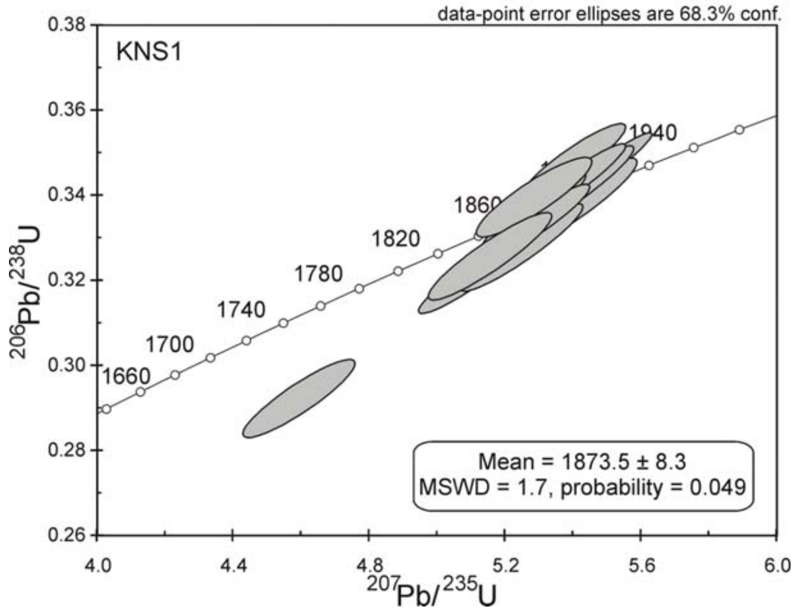

Figure 13: Concordia plot of zircon analyses for the Kinsenda Lufubu schist, sample KNS1.

Table 3. Summary of SHRIMP U-Th-Pb zircon results for sample KNS1.

							Radiogenic Ratios						Ages (in Ma)						
Grain. spot	U (ppm)	Th (ppm)	Th/U	Pb (ppm)	$^{204}Pb/^{206}Pb$	f_{206} %	$^{206}Pb/^{238}U$	±	$^{207}Pb/^{235}U$	±	$^{207}Pb/^{206}Pb$	±	$^{206}Pb/^{238}U$	±	$^{207}Pb/^{235}U$	±	$^{207}Pb/^{206}Pb$	±	Conc. %
1.1	218	315	1.44	98	0.00001	0.015	0.3367	0.0053	5.317	0.090	0.1145	0.0006	1871	25	1872	15	1872	9	100
2.1	173	181	1.05	74	0.00001	0.015	0.3480	0.0056	5.408	0.100	0.1127	0.0008	1925	27	1886	16	1843	13	104
3.1	176	192	1.09	74	0.00002	0.034	0.3379	0.0063	5.374	0.107	0.1154	0.0006	1877	30	1881	17	1885	9	100
4.1	186	213	1.14	80	0.00001	0.015	0.3447	0.0064	5.473	0.108	0.1151	0.0006	1909	31	1896	17	1882	9	101
5.1	203	260	1.28	87	0.00001	0.015	0.3339	0.0058	5.303	0.102	0.1152	0.0007	1857	28	1869	16	1883	11	99
6.1	88	97	1.10	37	0.00001	0.015	0.3371	0.0075	5.384	0.138	0.1158	0.0011	1873	36	1882	22	1893	18	99
7.1	134	124	0.93	51	0.00001	0.015	0.3209	0.0057	5.101	0.101	0.1153	0.0008	1794	28	1836	17	1884	13	95
7.2	194	193	1.00	70	0.00014	0.213	0.2924	0.0060	4.592	0.110	0.1139	0.0011	1654	30	1748	20	1863	18	89
8.1	108	145	1.35	48	0.00001	0.015	0.3410	0.0068	5.402	0.119	0.1149	0.0009	1892	33	1885	19	1878	13	101
9.1	136	164	1.20	56	0.00008	0.117	0.3276	0.0067	5.251	0.120	0.1163	0.0009	1827	33	1861	20	1899	14	96
10.1	196	238	1.21	84	0.00008	0.127	0.3429	0.0059	5.402	0.102	0.1143	0.0007	1900	28	1885	16	1869	11	102
11.1	200	256	1.28	87	0.00010	0.156	0.3394	0.0053	5.273	0.092	0.1127	0.0007	1884	26	1864	15	1843	11	102
12.1	190	163	0.86	75	0.00006	0.097	0.3361	0.0058	5.287	0.101	0.1141	0.0007	1868	28	1867	16	1865	12	100
13.1	245	253	1.03	100	0.00004	0.063	0.3339	0.0056	5.300	0.100	0.1151	0.0008	1857	27	1869	16	1882	12	99
14.1	145	149	1.03	60	0.00008	0.124	0.3393	0.0061	5.287	0.113	0.1130	0.0011	1883	30	1867	18	1848	17	102
15.1	163	184	1.13	66	0.00004	0.055	0.3256	0.0067	5.157	0.121	0.1149	0.0010	1817	33	1846	20	1878	16	97

Notes :

1. Uncertainties given at the one σ level.
2. f_{206} % denotes the percentage of ^{206}Pb that is common Pb.
3. Correction for common Pb made using the measured $^{204}Pb/^{206}Pb$ ratio.
4. For % Conc., 100% denotes a concordant analysis following Tera and Wasserburg (1972) as outlined in Compston et al. (1991).

Chambishi meta-trachyandesite (sample BN53/1)

Borehole BN53 is located in a prospect area called Mwambashi B, on the western flank of the Chambishi Basin (Figure 2). The total depth of this drill hole is 693.43 m, and the sample was collected from a depth of 685.35 m, ~20 m below the contact with basal Katangan sediments. BN53/1 is interpreted as a trachyandesitic metavolcanic quartz porphyry with relict deformed quartz and plagioclase phenocrysts (Table 1), which was transformed into a blastoporphyritic biotite-sericite schist (Figure 14). Ten zircons from BN53/1 were analysed (Table 4, Figure 15). The analyses plot in a single cluster and their weighted mean $^{207}Pb/^{206}Pb$ age is 1980 ± 7 Ma (MSWD = 0.55). This result is interpreted as the igneous age of the protolith volcanic rock.

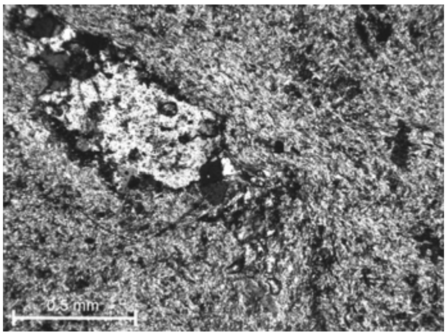

Figure 14: Photomicrograph of the Chambishi Lufubu schist, BN53/1.

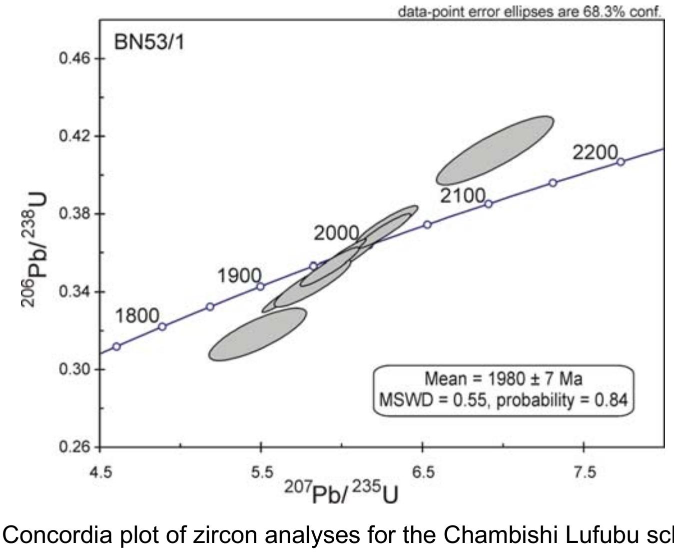

Figure 15: Concordia plot of zircon analyses for the Chambishi Lufubu schist, sample BN53/1.

Table 4. Summary of SHRIMP U-Th-Pb zircon results for sample BN53/1.

							Radiogenic Ratios						Ages (in Ma)						
Grain. spot	U (ppm)	Th (ppm)	Th/U	Pb (ppm)	$^{204}Pb/^{206}Pb$	f_{206} %	$^{206}Pb/^{238}U$	±	$^{207}Pb/^{235}U$	±	$^{207}Pb/^{206}Pb$	±	$^{206}Pb/^{238}U$	±	$^{207}Pb/^{235}U$	±	$^{207}Pb/^{206}Pb$	±	Conc. %
1.1	1210	877	0.72	443	0.00006	0.09	0.3186	0.0088	5.475	0.199	0.1246	0.0026	1783	43	1897	32	2023	37	88
2.1	197	113	0.58	90	0.00017	0.25	0.4121	0.0116	6.951	0.240	0.1223	0.0021	2224	53	2105	31	1991	30	112
3.1	492	340	0.69	189	0.00000	0.00	0.3385	0.0056	5.657	0.102	0.1212	0.0007	1879	27	1925	16	1974	10	95
4.1	374	275	0.74	148	0.00005	0.07	0.3447	0.0060	5.761	0.105	0.1212	0.0005	1909	29	1941	16	1974	7	97
5.1	248	156	0.63	100	0.00003	0.04	0.3575	0.0069	6.031	0.127	0.1223	0.0008	1970	33	1980	19	1991	12	99
6.1	284	185	0.65	119	0.00003	0.05	0.3739	0.0066	6.279	0.126	0.1218	0.0009	2048	31	2016	18	1983	14	103
7.1	346	352	1.02	146	0.00004	0.06	0.3447	0.0079	5.817	0.157	0.1224	0.0014	1909	38	1949	24	1991	21	96
8.1	221	167	0.76	95	0.00004	0.05	0.3711	0.0059	6.260	0.109	0.1223	0.0007	2034	28	2013	15	1991	10	102
9.1	380	366	0.96	164	0.00003	0.05	0.3582	0.0059	5.992	0.104	0.1213	0.0005	1974	28	1975	15	1976	7	100
10.1	232	163	0.70	93	0.00004	0.06	0.3530	0.0065	5.923	0.121	0.1217	0.0008	1949	31	1965	18	1981	12	98

Notes :
1. Uncertainties given at the one σ level.
2. f_{206} % denotes the percentage of ^{206}Pb that is common Pb.
3. Correction for common Pb made using the measured $^{204}Pb/^{206}Pb$ ratio.
4. For % Conc., 100% denotes a concordant analysis
   following Tera and Wasserburg (1972) as outlined in Compston et al. (1991).

Samba felsic metavolcanic schist (sample CT169/1256)

The Samba prospect is the largest copper deposit located in the basement of the Central African Copperbelt and consists of disseminations, stringers and veinlets of copper sulphides in quartz-sericite schists derived from porphyritic igneous rocks of quartz monzonite to granodioritic composition (Wakefield, 1978). Ore resources have been estimated at fifty million tons with an overall grade of about 0.5% Cu (Wakefield, 1978). The Samba prospect has been described by Wakefield (1978) as a porphyry-type deposit because of the presence of alteration zones, including a central sericitic core, as well as crackle-brecciation textures and the presence of chalcopyrite plus pyrite vein and disseminated mineralization (Figure 16).

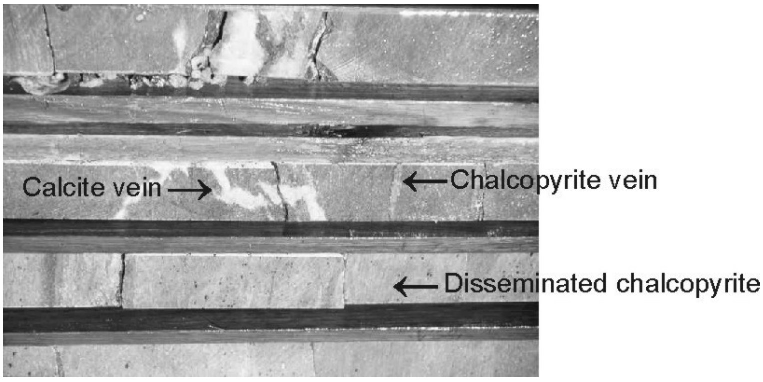

Figure 16: The Samba porphyry in split borehole. The core shows veins of calcite and chalcopyrite, and disseminated chalcopyrite in the altered porphyry.

The analysed sample is an epidotised biotite-muscovite-K-feldspar-quartz schist, interpreted as a felsic metavolcanic rock. A cathodoluminescence image (Figure 17) shows zircons with long axes < 200 μm. A striking feature of these zircons is the presence of irregular, low-uranium overgrowths. These overgrowths could not, however, be dated with the SHRIMP as they are smaller than the beam diameter. They could well be hydrothermal or metamorphic in origin, but their origin is still enigmatic. They resemble overgrowths of xenotime on zircons found in other samples from the Zambian Copperbelt (Hitzman, pers. comm., 2003). Although a few of the

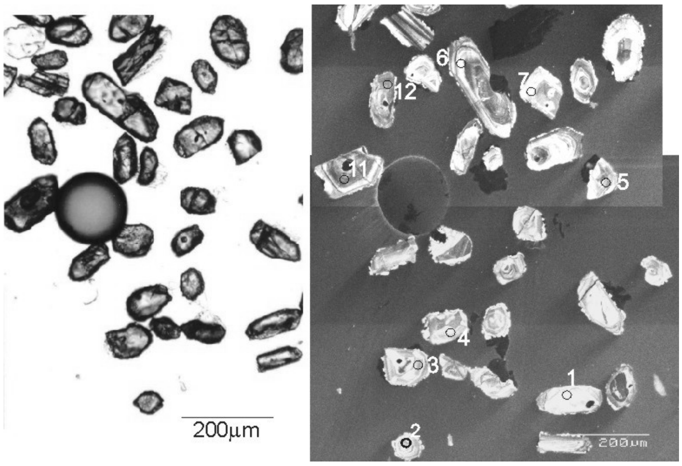

Figure 17: Photomicrograph and cathodoluminescence images of some of the analysed zircons, Samba.

zircons appear to be subrounded, the CL imagery shows that some of them are in fact euhedral zircons with the younger overgrowths. Sixteen analyses were performed on 16 zircons (Table 5, Figure 18). All but three analyses plot in a cluster which yielded a weighted mean $^{207}Pb/^{206}Pb$ age of 1964 ± 12 Ma (MSWD = 1.8). This result is interpreted as the emplacement age of the metavolcanic rock. Analyses 12.1, 13.1 and 16.1 gave older $^{207}Pb/^{206}Pb$ ages (2160 ± 25 Ma, 2336 ± 9 Ma and 2423 ± 13 Ma respectively). These three zircons are interpreted as xenocrystic.

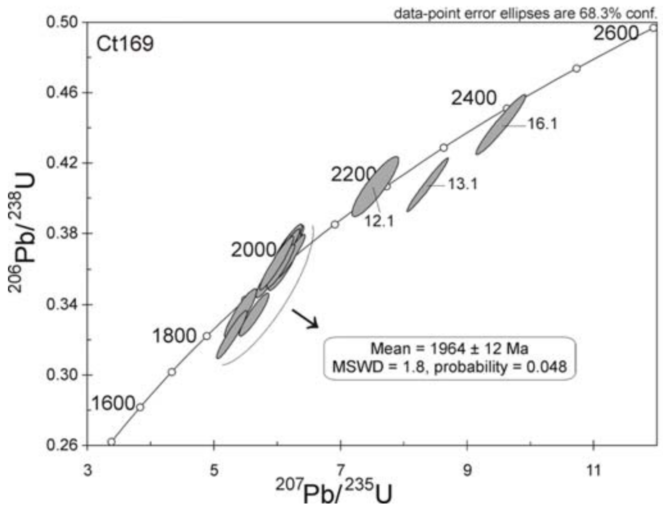

Figure 18: Concordia plot of zircon analyses for the Samba porphyry, sample CT169/1256.

Table 5. Summary of SHRIMP U-Th-Pb zircon results for sample CT169.

Grain. spot	U (ppm)	Th (ppm)	Th/U	Pb (ppm)	$^{204}Pb/^{206}Pb$	f_{206} %	Radiogenic Ratios $^{206}Pb/^{238}U$	±	$^{207}Pb/^{235}U$	±	$^{207}Pb/^{206}Pb$	±	Ages (in Ma) $^{206}Pb/^{238}U$	±	$^{207}Pb/^{235}U$	±	$^{207}Pb/^{206}Pb$	±	Conc. %
1.1	111	74	0.67	47	0.000202	0.31	0.3728	0.0080	6.170	0.159	0.1201	0.0014	2042	38	2000	23	1957	21	104
2.1	169	133	0.79	71	0.000029	0.04	0.3643	0.0072	6.062	0.134	0.1207	0.0009	2003	34	1985	20	1966	14	102
3.1	137	99	0.72	58	0.000170	0.26	0.3735	0.0078	6.162	0.147	0.1196	0.0011	2046	36	1999	21	1951	17	105
4.1	169	158	0.93	75	0.000002	0.00	0.3691	0.0072	6.170	0.129	0.1212	0.0006	2025	34	2000	18	1974	9	103
5.1	231	170	0.74	98	0.000048	0.07	0.3708	0.0078	6.133	0.143	0.1200	0.0009	2033	37	1995	20	1956	14	104
6.1	123	94	0.76	51	0.000015	0.02	0.3601	0.0077	6.071	0.151	0.1223	0.0013	1983	37	1986	22	1990	18	100
7.1	144	109	0.76	61	0.000020	0.03	0.3672	0.0079	6.202	0.148	0.1225	0.0010	2016	38	2005	21	1993	14	101
8.1	141	90	0.64	57	0.000069	0.10	0.3565	0.0081	5.877	0.153	0.1196	0.0012	1966	39	1958	23	1950	18	101
9.1	109	70	0.65	41	0.000130	0.20	0.3348	0.0081	5.621	0.154	0.1218	0.0013	1862	39	1919	24	1982	19	94
10.1	166	128	0.77	69	0.000041	0.06	0.3619	0.0080	6.048	0.148	0.1212	0.0010	1991	38	1983	22	1974	15	101
11.1	233	113	0.48	84	0.000277	0.44	0.3356	0.0091	5.408	0.169	0.1169	0.0015	1865	44	1886	27	1909	23	98
12.1*	168	73	0.43	74	0.000242	0.39	0.4065	0.0112	7.548	0.245	0.1347	0.0019	2199	51	2179	29	2160	25	102
13.1*	516	470	0.91	257	0.000100	0.16	0.4074	0.0100	8.378	0.215	0.1491	0.0008	2203	46	2273	24	2336	9	94
14.1	262	214	0.82	111	0.000111	0.18	0.3636	0.0098	5.984	0.177	0.1194	0.0011	1999	47	1973	26	1947	16	103
15.1	250	184	0.74	94	0.000161	0.26	0.3235	0.0089	5.272	0.161	0.1182	0.0012	1807	44	1864	26	1929	18	94
16.1*	404	334	0.83	213	0.000072	0.12	0.4413	0.0113	9.547	0.263	0.1569	0.0012	2356	51	2392	26	2423	13	97

Notes :

1. Uncertainties given at the one σ level.
2. f_{206} % denotes the percentage of ^{206}Pb that is common Pb.
3. Correction for common Pb made using the measured $^{204}Pb/^{206}Pb$ ratio.
4. For % Conc., 100% denotes a concordant analysis following Tera and Wasserburg (1972) as outlined in Compston et al. (1991).
5. * denotes analyses not included in the age calculation.

b. Granitoids and granitoid gneisses

Mkushi Gneiss (sample MGn)

First described by Bancroft and Pelletier (1929), Truter (1935) and Ackerman (1935, 1936), the banded to porphyroblastic biotitic granitoid Mkushi Gneiss was originally considered to be part of the Mkushi Group, comprising the Mkushi gneiss complex and some granites (Stillman,1965). De Waele and Mapani (2002) redefined the Mkushi Group as the "Mkushi Basement Complex" (MBC), which forms part of the basement to the southern Irumide belt in central Zambia and includes granitoid gneisses and granites. Jackson (1932) first correlated granitic gneisses of the Nchanga area on the Copperbelt with the Mkushi Gneisses from the Mkushi area, as defined by Bancroft and Pelletier (1929).

Field relations of the Mkushi Gneiss are complex and record several episodes of intrusion. The oldest intrusion is the biotite-bearing granite Mkushi Gneiss itself, which is strongly deformed and partly migmatitic. A second intrusive episode is represented by weakly deformed amphibolitic mafic dykes which cut across the foliation of the Mkushi Gneiss. Later undeformed aplite dykes, grading in places into pegmatites, are related to the Mtuga granite and cut both the Mkushi Gneiss and the mafic dykes (Stillman, 1965; N'gambi et al., 1986). The Mtuga aplites are mineralised and contain chalcopyrite and pyrite associated with rutile and sphene, with minor local bornite and traces of molybdenite (Omenetto, 1973, 1974; Legg, 1976). It is these bodies that have been exploited at the Mkushi copper mines, in the Munshiwemba open pit and the Mtuga underground operation, both of which ceased operations in the 1970's (Legg, 1976). Sample MGn comes from the typical Mkushi Gneiss exposed in the Munshiwemba open pit of the Mkushi copper mines (Figure 1 and 19).

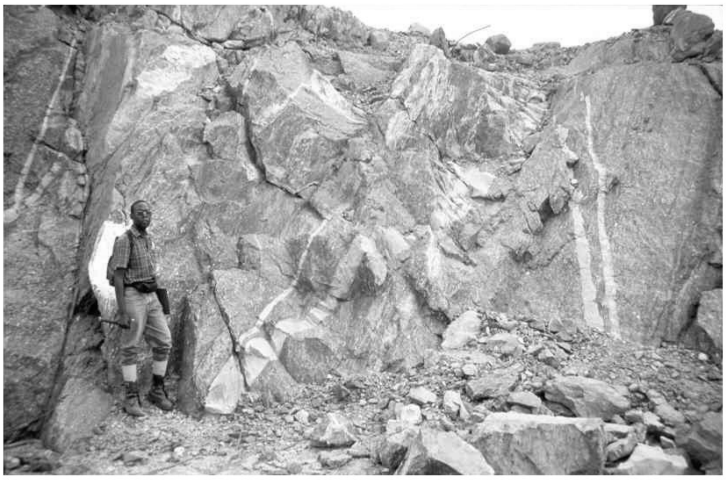

Figure 19: The Mkushi gneiss.

Twelve zircons were analysed (Table 6, Figure 20). The analyses plot in a single cluster and yield a weighted mean $^{207}Pb/^{206}Pb$ age of 2048.8 ± 5.8 Ma (MSWD = 0.85); excluding analysis 2.1 which is the most reversely discordant. This result is interpreted as the age of emplacement for the protolith of the Mkushi Gneiss.

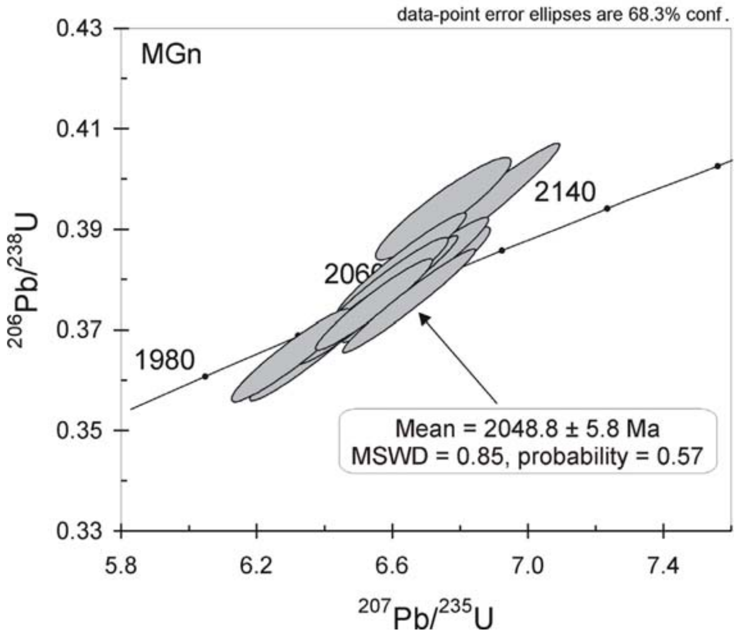

Figure 20: Concordia plot of zircon analyses for the Mkushi Gneiss, sample MGn

Table 6. Summary of SHRIMP U-Th-Pb zircon results for sample MGn.

							Radiogenic Ratios						Ages (in Ma)						
Grain. spot	U (ppm)	Th (ppm)	Th/U	Pb (ppm)	$^{204}Pb/^{206}Pb$	f_{206} %	$^{206}Pb/^{238}U$	±	$^{207}Pb/^{235}U$	±	$^{207}Pb/^{206}Pb$	±	$^{206}Pb/^{238}U$	±	$^{207}Pb/^{235}U$	±	$^{207}Pb/^{206}Pb$	±	Conc %
1.1	219	183	0.84	94	0.000017	0.03	0.3641	0.0064	6.344	0.119	0.1264	0.0006	2002	30	2025	17	2048	9	98
2.1	185	166	0.89	86	0.000050	0.08	0.3935	0.0069	6.742	0.133	0.1243	0.0009	2139	32	2078	18	2019	13	106
3.1	229	181	0.79	101	0.000001	-	0.3747	0.0070	6.639	0.130	0.1285	0.0005	2052	33	2065	17	2078	7	99
4.1	180	143	0.79	77	0.000091	0.14	0.3636	0.0062	6.287	0.117	0.1254	0.0007	1999	29	2017	16	2035	10	98
5.1	190	159	0.84	85	0.000007	0.01	0.3777	0.0065	6.571	0.123	0.1262	0.0007	2066	31	2055	17	2045	9	101
6.1	111	108	0.97	51	0.000001	-	0.3781	0.0077	6.658	0.148	0.1277	0.0009	2068	36	2067	20	2067	12	100
7.1	172	149	0.87	78	0.000025	0.04	0.3809	0.0071	6.676	0.133	0.1271	0.0007	2080	33	2069	18	2058	9	101
8.1	178	131	0.73	80	0.000029	0.04	0.3905	0.0108	6.793	0.196	0.1262	0.0007	2125	50	2085	26	2045	10	104
9.1	174	164	0.94	80	0.000033	0.05	0.3779	0.0067	6.596	0.124	0.1266	0.0006	2066	31	2059	17	2051	8	101
10.1	232	137	0.59	97	0.000018	0.03	0.3740	0.0061	6.536	0.116	0.1268	0.0006	2048	29	2051	16	2053	9	100
11.1	281	210	0.75	121	0.000004	0.01	0.3714	0.0062	6.481	0.117	0.1266	0.0006	2036	29	2043	16	2051	9	99
12.1	204	157	0.77	91	0.000117	0.18	0.3821	0.0069	6.616	0.128	0.1256	0.0006	2086	32	2062	17	2037	9	102

Notes :

1. Uncertainties given at the one σ level.
2. f_{206} % denotes the percentage of ^{206}Pb that is common Pb.
3. Correction for common Pb made using the measured $^{204}Pb/^{206}Pb$ ratio.
4. For % Conc., 100% denotes a concordant analysis following Tera and Wasserburg (1972) as outlined in Compston et al. (1991).

Mtuga aplites (samples APL-1 and APL-2)

Zircons from two mineralised Mtuga aplites (Figure 21) cutting the Mkushi gneiss were analysed.

Figure 21: The Mkushi Aplite crosscutting the foliation in the Mkushi Gneiss.

These aplites occur as pink- and cream-coloured intrusions and are post-tectonic relative to the deformation and metamorphism that affected the host gneisses. Fourteen zircons from sample APL-1 were analysed (Table 7, Figure 22). Most of the zircons observed were distinctly zoned, comprising cores and thin rims that were to small to analyse.

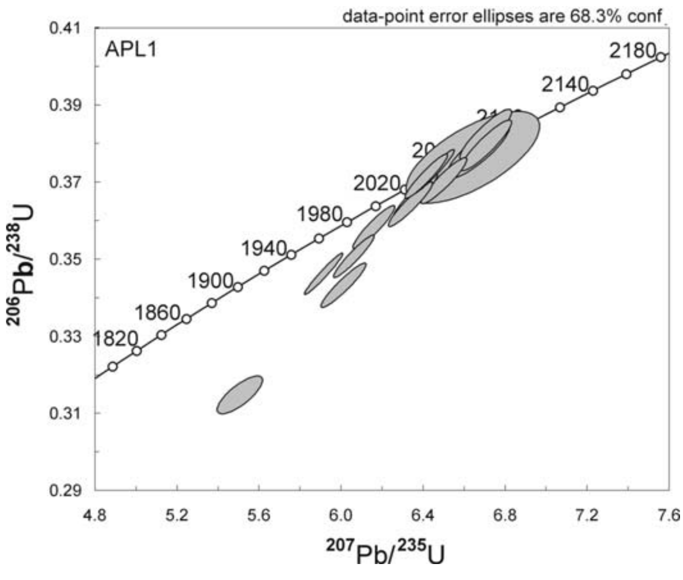

Figure 22: Concordia plot of zircon analyses for the Mtuga aplite, sample APL1.

Table 7. Summary of SHRIMP U-Th-Pb zircon results from sample APL1

Grain.	U	Th	Th/U	Pb	^{204}Pb/	f_{206}	Radiogenic Ratios						Ages (in Ma)						Conc.
							^{206}Pb/		^{207}Pb/		^{207}Pb/		^{206}Pb/		^{207}Pb/		^{207}Pb/		
spot	(ppm)	(ppm)		(ppm)	^{206}Pb	%	^{238}U	±	^{235}U	±	^{206}Pb	±	^{238}U	±	^{235}U	±	^{206}Pb	±	%
APL-1																			
1.1	178	114	0.64	76	0.00000	0.00	0.3782	0.0047	6.661	0.102	0.1277	0.0010	2068	22	2068	14	2067	13	100
2.1	361	409	1.13	140	0.00009	0.13	0.3434	0.0037	5.997	0.072	0.1267	0.0005	1903	18	1975	11	2052	7	93
3.1	176	174	0.99	81	0.00001	0.02	0.3764	0.0078	6.635	0.217	0.1278	0.0029	2060	37	2064	29	2068	41	100
4.1	612	387	0.65	167	0.00049	0.73	0.3151	0.0032	5.487	0.072	0.1263	0.0010	1766	16	1899	11	2047	15	86
5.1	657	308	0.48	198	0.00002	0.04	0.3509	0.0036	6.047	0.066	0.1250	0.0004	1939	17	1983	9	2029	6	96
6.1	477	284	0.62	147	0.00004	0.06	0.3584	0.0037	6.147	0.068	0.1244	0.0005	1975	17	1997	10	2020	7	98
7.1	192	193	1.04	63	0.00003	0.05	0.3822	0.0043	6.698	0.084	0.1271	0.0007	2087	20	2072	11	2058	10	101
8.1	338	91	0.28	106	0.00004	0.05	0.3664	0.0039	6.353	0.072	0.1258	0.0005	2012	18	2026	10	2040	7	99
9.1	639	462	0.75	204	0.00010	0.15	0.3715	0.0038	6.408	0.069	0.1251	0.0004	2037	18	2033	9	2030	6	100
10.1	829	149	0.19	247	0.00000	0.00	0.3462	0.0035	5.902	0.061	0.1236	0.0003	1916	17	1962	9	2009	4	95
11.1	577	362	0.65	185	0.00003	0.04	0.3726	0.0038	6.440	0.069	0.1254	0.0004	2042	18	2038	9	2034	5	100
12.1	400	530	1.37	125	0.00005	0.08	0.3643	0.0038	6.329	0.071	0.1260	0.0005	2002	18	2022	10	2043	7	98
13.1	322	269	0.86	103	0.00004	0.06	0.3705	0.0039	6.494	0.074	0.1271	0.0006	2032	18	2045	10	2059	8	99
14.1	189	110	0.60	62	0.00001	0.00	0.3794	0.0043	6.700	0.083	0.1281	0.0007	2074	20	2073	11	2072	9	100

Notes :

1. Uncertainties given at the one σ level.
2. f_{206} % denotes the percentage of ^{206}Pb that is common Pb.
3. For % Conc., 100% denotes a concordant analysis following Tera and Wasserburg (1972) as outlined in Compston et al. (1991).

Ages for APL-1 were only obtained from cores, which show a range in $^{206}Pb/^{207}Pb$ ages from 2072 ± 9 Ma to 2009 ± 4 Ma. These cores are interpreted as xenocrystic. Nineteen cores and twelve rims of zircons from sample APL-2 were also analysed (Table 8, Figure 23). High–uranium zircon rims yielded a significantly younger $^{207}Pb/^{206}Pb$ age of 1059 ± 26 Ma (mean of 10 analyses) shown as an upper intercept in Figure 22. This age is interpreted as the age of intrusion of the aplites. They are related to the emplacement of other Irumide granitoids that are known to occur in the area and have yielded SHRIMP zircon ages of 1050-950 Ma (de Waele et al., 2003).

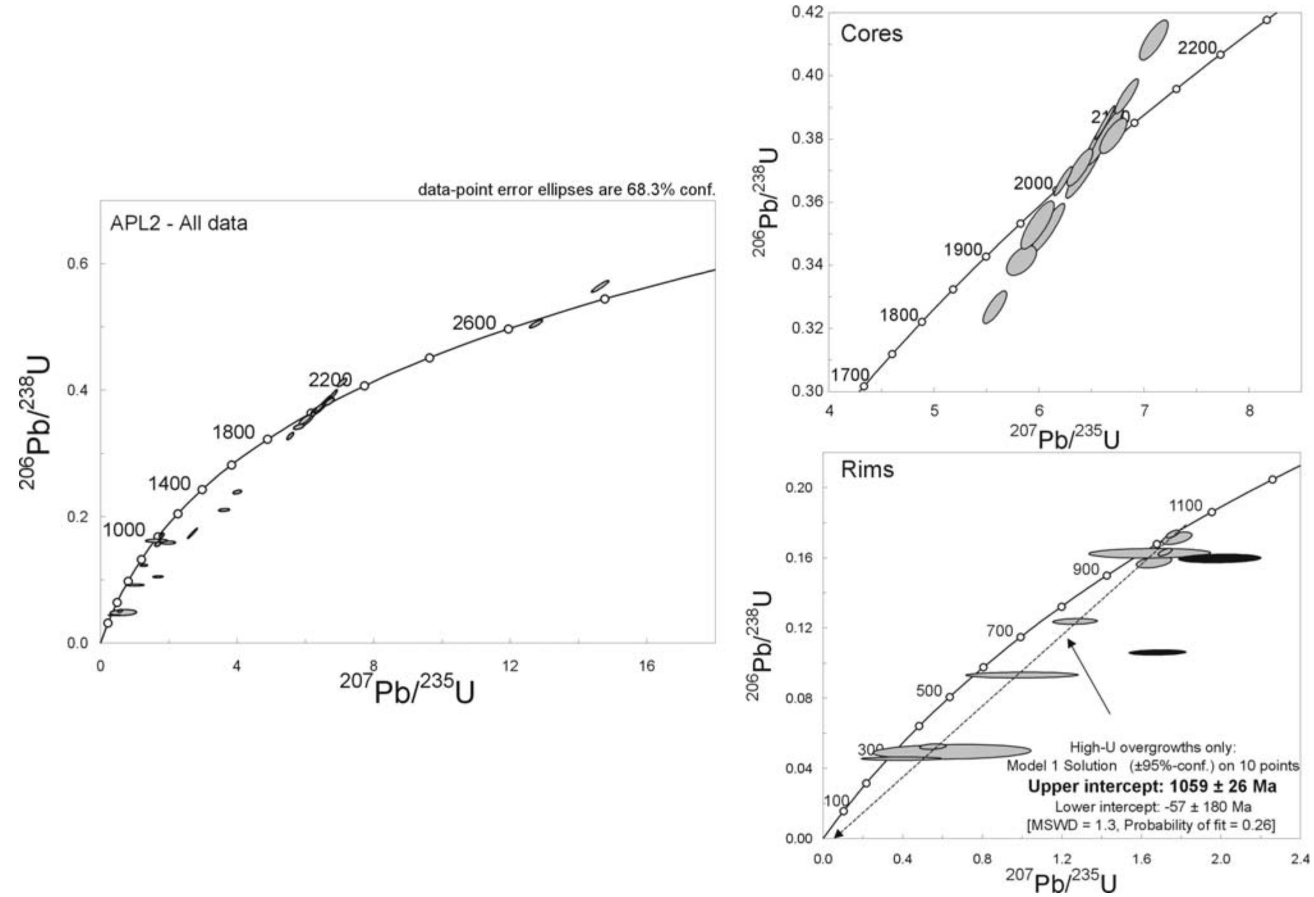

Figure 23: Concordia plot of zircon analyses forf the Mtuga aplite, sample APL2. Dark ellipses – Low-U overgrowths.

Table 8. Summary of SHRIMP U-Th-Pb zircon results for sample APL2

							Radiogenic Ratios						Ages (in Ma)						
Grain. spot	U (ppm)	Th (ppm)	Th/U	Pb (ppm)	$^{204}Pb/^{206}Pb$	f_{206} %	$^{206}Pb/^{238}U$	±	$^{207}Pb/^{235}U$	±	$^{207}Pb/^{206}Pb$	±	$^{206}Pb/^{238}U$	±	$^{207}Pb/^{235}U$	±	$^{207}Pb/^{206}Pb$	±	Conc. %
1.1c	171	88	0.52	69	0.000028	0.04	0.3703	0.0060	6.422	0.118	0.1258	0.0009	2031	28	2035	16	2040	12	100
1.2r	1433	184	0.13	83	0.033820	50.4	0.0492	0.0028	0.646	0.261	0.0952	0.0375	310	17	506	176	1531	1013	20
2.1	177	80	0.45	73	0.000255	0.38	0.3810	0.0059	6.603	0.117	0.1257	0.0009	2081	27	2060	16	2039	13	102
4.1r	1687	66	0.04	89	0.010577	15.8	0.0523	0.0011	0.550	0.044	0.0763	0.0057	329	6	445	29	1102	158	30
5.1c	244	103	0.42	92	0.000253	0.38	0.3517	0.0052	6.068	0.103	0.1251	0.0009	1943	25	1986	15	2031	12	96
6.1r	1498	294	0.20	252	0.000605	0.9	0.1742	0.0052	2.690	0.086	0.1120	0.0009	1035	29	1326	24	1832	14	57
9.1r	992	279	0.28	157	0.001869	2.8	0.1574	0.0022	1.663	0.058	0.0766	0.0023	942	12	994	22	1111	62	85
9.2r	968	275	0.28	167	0.006061	9.0	0.1714	0.0024	1.779	0.049	0.0753	0.0017	1020	13	1038	18	1076	45	95
11.1c	831	91	0.11	173	0.001116	1.70	0.2388	0.0021	4.009	0.078	0.1218	0.0021	1380	11	1636	16	1982	31	30
12.1c	175	55	0.32	57	0.000014	0.02	0.3807	0.0060	6.621	0.111	0.1261	0.0007	2080	28	2062	15	2045	10	-2
13.1c	633	87	0.14	179	0.000381	0.58	0.3268	0.0034	5.563	0.073	0.1235	0.0010	1823	17	1910	11	2007	14	9
14.1c	1198	53	0.05	519	0.000062	0.08	0.5037	0.0041	12.772	0.120	0.1839	0.0009	2630	17	2663	9	2688	8	2
15.1c	173	71	0.42	57	0.000172	0.26	0.3810	0.0037	6.697	0.086	0.1275	0.0011	2081	17	2072	11	2064	15	-1
16.1c	278	130	0.48	82	0.000460	0.70	0.3415	0.0031	5.819	0.096	0.1236	0.0017	1894	15	1949	14	2009	24	6
16.2c	197	54	0.28	63	0.000162	0.25	0.3709	0.0039	6.377	0.080	0.1247	0.0009	2034	18	2029	11	2024	12	0

Notes :

1. Uncertainties given at the one σ level.
2. f_{206} % denotes the percentage of ^{206}Pb that is common Pb.
3. Correction for common Pb made using the measured $^{204}Pb/^{206}Pb$ ratio.
4. C = core; r = rim; e = embayment
5. For % Conc., 100% denotes a concordant analysis following Tera and Wasserburg (1972) as outlined in Compston et al. (1991).

Table 8. Summary of SHRIMP U-Th-Pb zircon results for sample APL2

Grain. spot	U (ppm)	Th (ppm)	Th/U	Pb (ppm)	$^{204}Pb/^{206}Pb$	f_{206} %	Radiogenic Ratios $^{206}Pb/^{238}U$	±	$^{207}Pb/^{235}U$	±	$^{207}Pb/^{206}Pb$	±	Ages (in Ma) $^{206}Pb/^{238}U$	±	$^{207}Pb/^{235}U$	±	$^{207}Pb/^{206}Pb$	±	Conc. %
17.1e	802	39	0.05	253	0.000093	0.14	0.3666	0.0030	6.216	0.055	0.1230	0.0004	2013	14	2007	8	2000	6	-1
17.2r	199	151	0.78	67	0.000043	0.06	0.3935	0.0037	6.826	0.072	0.1258	0.0006	2139	17	2089	9	2040	9	-5
18.1c	1104	122	0.11	203	0.001001	1.51	0.2111	0.0018	3.615	0.108	0.1242	0.0036	1235	10	1553	23	2017	51	39
18.2r	1872	93	0.05	169	0.006742	11.33	0.0931	0.0011	0.999	0.187	0.0779	0.0145	574	6	704	91	1144	370	50
19.1r	2937	208	0.07	136	0.008996	15.82	0.0455	0.0006	0.392	0.132	0.0625	0.0210	287	4	336	92	692	716	59
19.2c	128	68	0.55	39	0.000289	0.44	0.3527	0.0050	5.973	0.104	0.1228	0.0012	1947	24	1972	15	1998	18	3
20.1e	1262	9	0.01	418	0.000038	0.06	0.3851	0.0035	6.615	0.062	0.1246	0.0003	2100	16	2061	8	2023	4	-4
9.3r	1409	348	0.26	211	0.000214	0.36	0.1737	0.0014	1.756	0.021	0.0733	0.0007	1032	8	1029	8	1023	18	-1
9.4r	1624	436	0.28	242	0.003679	6.27	0.1626	0.0018	1.642	0.202	0.0732	0.0090	971	10	986	75	1020	249	5
20.2c	124	89	0.74	44	0.000029	0.04	0.4113	0.0041	7.081	0.091	0.1249	0.0010	2221	19	2122	11	2027	14	-10
21.1c	1731	430	0.26	166	0.003201	4.93	0.1061	0.0009	1.680	0.094	0.1149	0.0063	650	6	1001	35	1878	99	65
22.1c	300	161	0.55	145	0.000000	0.00	0.5622	0.0059	14.622	0.166	0.1886	0.0008	2876	24	2791	11	2730	7	-5
23.1r	1383	28	0.02	195	0.000251	0.42	0.1633	0.0014	1.719	0.023	0.0764	0.0008	975	8	1016	9	1105	20	12
24.1r	1252	92	0.08	138	0.002094	3.56	0.1238	0.0011	1.265	0.074	0.0741	0.0043	752	6	830	33	1045	117	28
25.1c	1106	195	0.18	156	0.001543	2.51	0.1597	0.0016	1.995	0.138	0.0906	0.0062	955	9	1114	46	1438	130	34

Notes :

1. Uncertainties given at the one σ level.
2. f_{206} % denotes the percentage of ^{206}Pb that is common Pb.
3. Correction for common Pb made using the measured $^{204}Pb/^{206}Pb$ ratio.
4. C = core; r = rim; e = embayment
5. For % Conc., 100% denotes a concordant analysis following Tera and Wasserburg (1972) as outlined in Compston et al. (1991).

Mufulira Pink Granite (sample MPG)

Two distinct phases of granitoids are present in the vicinity of the Mufulira Mine (Brandt et al., 1961). The western Mufulira Grey Granodiorite, which is the most abundant, is uniformly grey and is characterised by xenoliths of Lufubu schist (Brandt et al., 1961; Cahen et al., 1970c). This is a typical biotite granodiorite (also called a tonalite by Darnley, 1960) comprising epidote, plagioclase, quartz, biotite (sometimes altered to chlorite), scarce muscovite, magnetite, ilmenite and sphene. The pink granite comprises microcline, quartz, scarce plagiocase, and abundant muscovite (but no biotite or epidote) together with magnetite, rutile and haematite as accessory minerals. This granite lacks xenoliths of Lufubu schist. Ten zircons from the Mufulira Pink Granite were analysed (Table 9, Figure 24). The analyses plot along a discordia with an upper intercept of 1993.7 ± 7.1 Ma (MSWD = 1.05), interpreted as the emplacement age. The discordant data may reflect a Pb-loss of Pb during a Pan-African metamorphic event or during recent weathering. The ages of the Mufulira Lufubu schists (1968 Ma) and the Mufulira Pink Granite, together with the fact that the Mufulira Grey Granodiorite contains xenoliths of Lufubu schists, indicate that the pink and grey granites are two separate intrusions emplaced at significantly different times. The Grey Granodiorite may be ca. 1945 Ma in age following model 1 of Cahen et al.,1970c (see above).

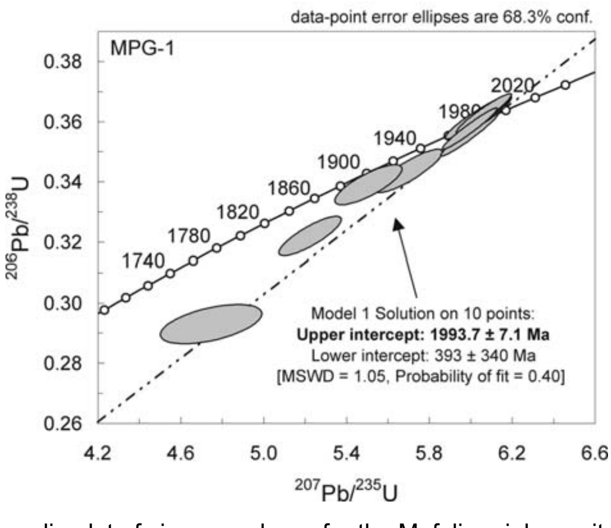

Figure 24: Concordia plot of zircon analyses for the Mufulira pink granite, sample MPG

Table 9. Summary of SHRIMP U-Th-Pb zircon results for sample MPG-1.

							Radiogenic Ratios						Ages (in Ma)						
Grain. spot	U (ppm)	Th (ppm)	Th/U	Pb (ppm)	$^{204}Pb/^{206}Pb$	f_{206} %	$^{206}Pb/^{238}U$	±	$^{207}Pb/^{235}U$	±	$^{207}Pb/^{206}Pb$	±	$^{206}Pb/^{238}U$	±	$^{207}Pb/^{235}U$	±	$^{207}Pb/^{206}Pb$	±	Conc. %
1.1	667	426	0.64	270	0.000031	0.05	0.3615	0.0045	6.1059	0.0805	0.1225	0.0004	1989	21	1991	12	1993	6	100
2.1	702	468	0.67	280	0.000183	0.32	0.3619	0.0043	6.0985	0.0843	0.1222	0.0007	1991	21	1990	12	1989	10	100
3.1	303	259	0.86	99	0.003630	6.27	0.2933	0.0044	4.9163	0.1449	0.1216	0.0029	1658	22	1805	25	1979	43	84
4.1	398	188	0.47	153	0.000021	0.04	0.3557	0.0046	6.0393	0.0839	0.1232	0.0004	1962	22	1982	12	2002	6	98
5.1	553	338	0.61	220	0.000309	0.54	0.3606	0.0043	6.0577	0.0804	0.1218	0.0006	1985	20	1984	12	1983	8	100
6.1	580	281	0.49	228	0.000017	0.03	0.3626	0.0043	6.1048	0.0792	0.1221	0.0005	1994	20	1991	11	1988	7	100
7.1	566	395	0.70	230	0.000032	0.06	0.3576	0.0043	6.0436	0.0776	0.1226	0.0004	1971	20	1982	11	1994	6	99
8.1	495	280	0.56	184	0.000396	0.69	0.3391	0.0044	5.6023	0.0960	0.1198	0.0012	1882	21	1917	15	1954	18	96
9.1	548	302	0.55	207	0.000577	1.00	0.3436	0.0047	5.7758	0.0955	0.1219	0.0010	1904	22	1943	14	1984	14	96
10.1	444	220	0.49	156	0.000630	1.09	0.3222	0.0043	5.3512	0.0889	0.1204	0.0010	1801	21	1877	14	1963	15	92

Notes :

1. Uncertainties given at the one σ level.
2. f_{206} % denotes the percentage of ^{206}Pb that is common Pb.
3. Correction for common Pb made using the measured $^{204}Pb/^{206}Pb$ ratio.
4. For % Conc., 100% denotes a concordant analysis
   following Tera and Wasserburg (1972) as outlined in Compston et al. (1991).

Chambishi Granite (sample NN75/1)

Borehole NN75 is located in the Chambishi South-East prospect 13 km NE of drill hole BN53. The total depth of bore hole NN75 is 1033.78m, and our sample was collected from a depth of 1030.31m, 14 m below the nonconformable contact between the basal Roan Group sediments of the Katanga Supergroup, and an underlying granite which we call the Chambishi Granite. Sample NN75/1 is a medium- to coarse-grained, weakly foliated biotite granite (Table 10, Figure 25).

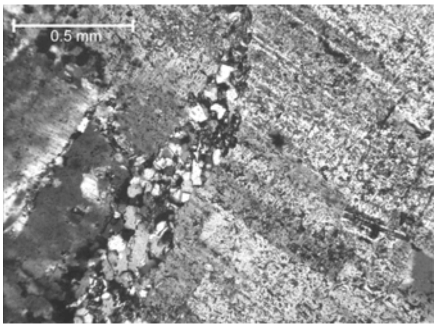

Figure 25: Photomicrograph of Chambishi granite, sample NN75/1.

Fifteen zircons from NN75/1 were analysed (Table 11, Figure 26). The analyses plot in a single cluster, yielding a weighted mean $^{207}Pb/^{206}Pb$ age of 1983 ± 5 Ma (MSWD = 1.12). This result is interpreted as the emplacement age of the Chambishi Granite.

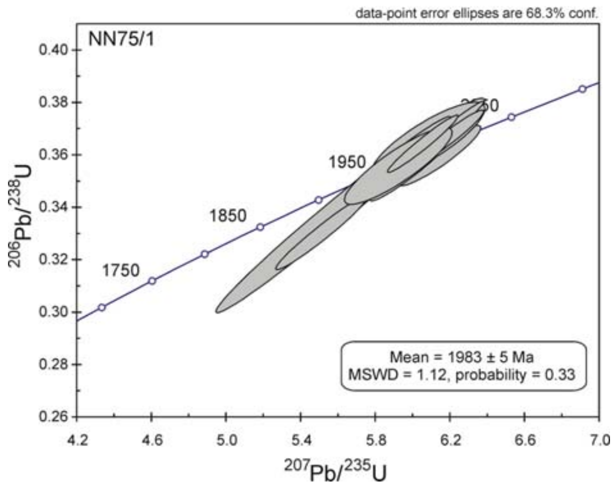

Figure 26: Concordia plot of zircon analyses for the Chambishi granite, sample NN75/1.

Table 10: Chemical analyses, sample NN75/1

Sample Number	ppm Rb	ppm Sr	ppm Y	ppm Zr	ppm Nb	ppm Co	ppm Ni	ppm Cu	ppm Zn	%TiO2	ppm V	ppm Cr	ppm Ba
LLD	**3**	**3**	**3**	**8**	**3**	**6**	**6**	**6**	**6**	**0.01**	**12**	**12**	**10**
NN 75/1	107	210	21	123	12	28	12	<9	46	0.44	44	17	1146

Sample Number	%SiO2	%TiO2	%Al2O3	%Fe2O3	%MnO	%MgO	%CaO	%Na2O	%K2O	%P2O5	%LOI	%TOTAL
NN 75/1	69.47	0.40	14.21	2.97	0.07	1.65	1.58	4.62	3.38	0.09	1.21	99.64

Table 11. Summary of SHRIMP U-Th-Pb zircon results for sample NN75/1.

							Radiogenic Ratios						Ages (in Ma)						
Grain. spot	U (ppm)	Th (ppm)	Th/U	Pb (ppm)	$^{204}Pb/^{206}Pb$	f_{206} %	$^{206}Pb/^{238}U$	±	$^{207}Pb/^{235}U$	±	$^{207}Pb/^{206}Pb$	±	$^{206}Pb/^{238}U$	±	$^{207}Pb/^{235}U$	±	$^{207}Pb/^{206}Pb$	±	Conc. %
1.1	252	248	0.98	111	0.000005	0.01	0.3637	0.0070	6.128	0.124	0.1222	0.0005	2000	33	1994	18	1988	8	101
2.1	290	218	0.75	118	0.000019	0.03	0.3539	0.0066	5.980	0.121	0.1226	0.0008	1953	31	1973	18	1994	11	98
2.2	81	50	0.62	33	0.000010	0.02	0.3596	0.0076	6.142	0.149	0.1239	0.0012	1980	36	1996	21	2013	17	98
3.1	336	291	0.87	144	0.000047	0.07	0.3633	0.0067	6.081	0.123	0.1214	0.0008	1998	32	1988	18	1977	11	101
4.1	198	144	0.73	80	0.000005	0.01	0.3543	0.0078	5.988	0.142	0.1226	0.0008	1955	37	1974	21	1994	12	98
5.1	178	128	0.72	75	0.000016	0.02	0.3702	0.0073	6.184	0.136	0.1212	0.0010	2031	34	2002	19	1973	14	103
5.2	111	63	0.57	45	0.000093	0.14	0.3653	0.0096	6.084	0.202	0.1208	0.0021	2007	45	1988	29	1968	31	102
6.1	192	111	0.58	72	0.000078	0.12	0.3372	0.0245	5.575	0.418	0.1199	0.0014	1873	119	1912	67	1955	20	96
7.1	279	192	0.69	105	0.000088	0.13	0.3302	0.0092	5.510	0.162	0.1210	0.0008	1839	45	1902	26	1972	12	93
8.1	266	200	0.75	111	0.000026	0.04	0.3609	0.0071	6.080	0.125	0.1222	0.0005	1987	34	1987	18	1988	7	100
9.1	474	406	0.86	203	0.000022	0.03	0.3640	0.0066	6.141	0.118	0.1224	0.0005	2001	31	1996	17	1991	7	101
10.1	235	155	0.66	96	0.000062	0.09	0.3616	0.0067	6.033	0.121	0.1210	0.0007	1990	32	1981	18	1971	10	101
11.1	226	174	0.77	92	0.000027	0.04	0.3535	0.0066	5.923	0.117	0.1215	0.0006	1951	31	1965	17	1978	9	99
12.1	264	202	0.77	110	0.000003	0.01	0.3631	0.0112	6.091	0.195	0.1217	0.0006	1997	53	1989	28	1981	9	101
13.1	172	186	1.08	78	0.000025	0.04	0.3663	0.0070	6.193	0.127	0.1226	0.0007	2012	33	2003	18	1995	10	101
14.1	155	99	0.64	62	0.000024	0.04	0.3556	0.0096	5.924	0.191	0.1208	0.0018	1961	46	1965	28	1968	27	100
15.1	228	171	0.75	95	0.000028	0.04	0.3640	0.0071	6.057	0.125	0.1207	0.0006	2001	34	1984	18	1966	9	102

Notes :
1. Uncertainties given at the one s level.
2. f_{206} % denotes the percentage of ^{206}Pb that is common Pb.
3. Correction for common Pb made using the measured $^{204}Pb/^{206}Pb$ ratio.
4. For % Conc., 100% denotes a concordant analysis following Tera and Wasserburg (1972) as outlined in Compston et al. (1991).

Mulungushi Bridge augen gneiss (sample MFG-1)

Sample MFG-1 is a megacrystic augen orthogneiss from the Mulungushi Bridge ca 20 km N of Kabwe (Figure 1 and 27). It forms part of the basement to the Irumide Belt, and contains a strong foliation, defined by biotite, which trends NNE-SSW, parallel to the trend of the Irumide Belt. Twelve zircons from the augen gneiss were analysed (Table 12, Figure 28). The analysed zircons form a cluster which yielded a weighted mean $^{207}Pb/^{206}Pb$ age of 1976.2 ± 4.8 Ma (MSWD = 0.87). There are three main possibilities of the origin for the zircons which have been analysed from this sample: magmatic, magmatic with a metamorphic overgrowth rim, and completely metamorphic. Since the ages of all zircons analysed plot in a cluster, the possibility that the zircons are of magmatic origin with a metamorphic rim may be dismissed. Other samples of intrusives described in this paper give a range of ages of 2050-1960 Ma, with none showing any metamorphic influence at this time. The ages obtained from sample MFG-1 plot well within this range. The preferred interpretation of the age 1976 Ma is that it represents the emplacement of the Mulungushi gneiss protolith.

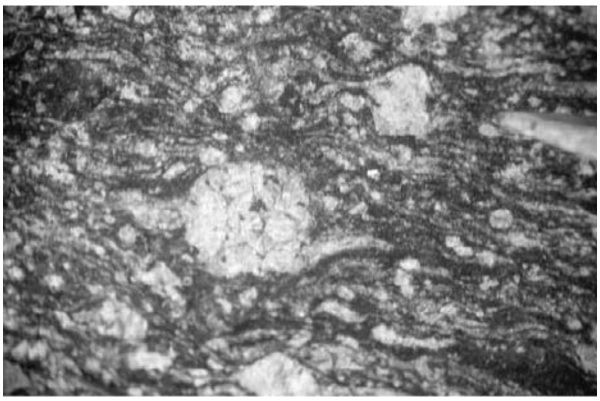

Figure 27: the Mulungushi Bridge augen gneiss.

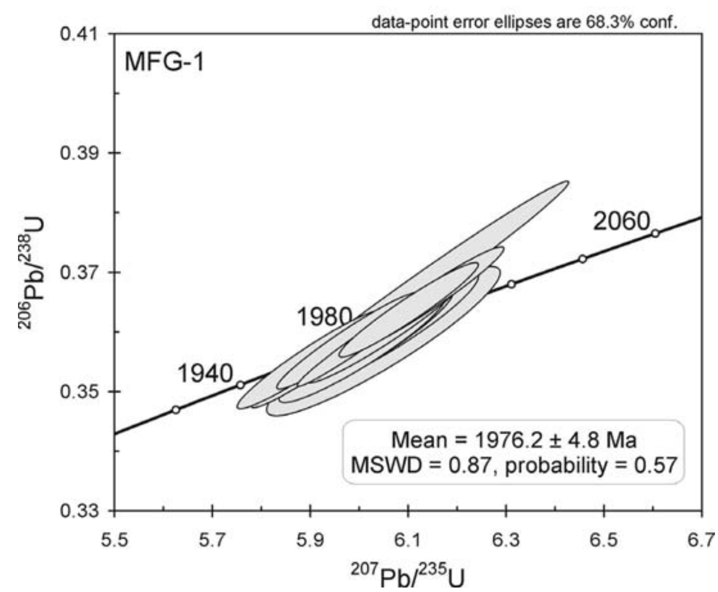

Figure 28: Concordia plot of zircon analyses for the Mulungushi Bridge augen gneiss, sample MFG-1.

Table 12. Summary of SHRIMP U-Th-Pb zircon results for sample MFG-1.

							Radiogenic Ratios						Ages (in Ma)						
Grain. spot	**U (ppm)**	**Th (ppm)**	**Th/U**	**Pb (ppm)**	**$^{204}Pb/^{206}Pb$**	**f_{206} %**	**$^{206}Pb/^{238}U$**	**±**	**$^{207}Pb/^{235}U$**	**±**	**$^{207}Pb/^{206}Pb$**	**±**	**$^{206}Pb/^{238}U$**	**±**	**$^{207}Pb/^{235}U$**	**±**	**$^{207}Pb/^{206}Pb$**	**±**	Conc. **%**
1.1	135	145	1.07	61	0.000009	0.01	0.3668	0.0122	6.110	0.209	0.1208	0.0006	2014	58	1992	30	1969	8	102
2.1	123	87	0.71	51	0.000060	0.09	0.3601	0.0065	6.055	0.124	0.1220	0.0009	1983	31	1984	18	1985	14	100
3.1	70	69	0.99	30	0.000010	0.02	0.3570	0.0060	6.003	0.112	0.1219	0.0008	1968	29	1976	16	1985	11	99
4.1	288	344	1.20	130	0.000015	0.02	0.3590	0.0054	6.013	0.095	0.1215	0.0004	1977	26	1978	14	1978	5	100
5.1	58	45	0.77	24	0.000051	0.08	0.3583	0.0083	6.046	0.159	0.1224	0.0012	1974	39	1983	23	1991	18	99
6.1	143	118	0.83	59	0.000034	0.05	0.3553	0.0054	5.895	0.098	0.1204	0.0006	1960	26	1961	15	1962	8	100
7.1	146	141	0.96	63	0.000049	0.07	0.3604	0.0060	6.051	0.109	0.1218	0.0006	1984	29	1983	16	1982	9	100
8.1	161	146	0.91	68	0.000049	0.07	0.3561	0.0059	5.933	0.104	0.1208	0.0005	1964	28	1966	15	1969	7	100
9.1	186	138	0.75	76	0.000022	0.03	0.3584	0.0054	5.974	0.096	0.1209	0.0005	1974	26	1972	14	1970	8	100
10.1	105	106	1.00	46	0.000029	0.04	0.3580	0.0061	6.018	0.114	0.1219	0.0008	1973	29	1978	17	1985	12	99
11.1	155	137	0.89	67	0.000042	0.06	0.3655	0.0057	6.138	0.103	0.1218	0.0005	2008	27	1996	15	1983	7	101
12.1	245	144	0.59	99	0.000033	0.05	0.3636	0.0053	6.099	0.095	0.1217	0.0005	1999	25	1990	14	1981	8	101

Notes :

1. Uncertainties given at the one σ level.
2. f_{206} % denotes the percentage of ^{206}Pb that is common Pb.
3. Correction for common Pb made using the measured $^{204}Pb/^{206}Pb$ ratio.
4. For % Conc., 100% denotes a concordant analysis following Tera and Wasserburg (1972) as outlined in Compston et al. (1991).

c. Basement ages from xenocrystic zircons in the Katanga Supergroup

Roan Group tuff (sample Etoile 1)

The Mine de l'Etoile du Congo or "Star of the Congo Mine" is located 12 Km NE of Lubumbashi (DRC). The deposit was inferred by Lefebvre and Cailteux (1975) to be hosted within a thrust slice of the Roan Group, but has been reinterpreted by Wendorff (2003) to occur within olistostromal megaclasts of former Roan Group rocks within the syntectonic Fungurume Group. There is no outcrop of the basement, which is buried under kilometres of tectonically-thickened Katangan rocks. Tuffs occur within the lower part of the Roan Group and more particularly within the beds of the Serie des Mines, known locally as the red RAT, SD and CMN (Machairas, 1974; Auger, 1975; Lefebvre and Cailteux, 1975). Sample Etoile 1 is a dolomitic carbonate rock with interbedded thin graded layers (~ 1 mm thick) of primarily iron oxides and devitrified shards interpreted as volcanic tuff horizons (Figure 29). The sample was collected to constraint the age of the volcanism but only three zircons were found, which yielded $^{207}Pb/^{206}Pb$ ages of 2831 ± 16 Ma, 2802 ± 36 and 1858 ± 24 Ma (Table 13). These ages are older than the maximum age of deposition of the Katangan sequence (880 Ma) and the three analysed zircons are inferred to be xenocrystics.

Figure 29: Photomicrograph of Katangan tuff sample Etoile 1.

Table 13. Summary of SHRIMP U-Th-Pb results for Etoile detrital zircons.

							Radiogenic Ratios						Ages (in Ma)						
Grain. spot	U (ppm)	Th (ppm)	Th/U	Pb (ppm)	$^{204}Pb/^{206}Pb$	f_{206} %	$^{206}Pb/^{238}U$	±	$^{207}Pb/^{235}U$	±	$^{207}Pb/^{206}Pb$	±	$^{206}Pb/^{238}U$	±	$^{207}Pb/^{235}U$	±	$^{207}Pb/^{206}Pb$	±	Conc. %
1.1	151	144	0.96	60	0.00018	0.333	0.3339	0.0152	5.231	0.256	0.1136	0.0015	1857	74	1858	43	1858	24	100
2.1	83	199	2.40	77	0.00033	0.612	0.5874	0.0305	16.242	0.878	0.2006	0.0020	2979	125	2891	53	2831	16	105
3.1	21	65	3.13	21	0.00036	0.677	0.5705	0.0350	15.498	1.049	0.1970	0.0043	2910	145	2846	67	2802	36	104

Notes :

1. Uncertainties given at the one σ level.
2. f_{206} % denotes the percentage of ^{206}Pb that is common Pb.
3. Correction for common Pb made using the measured $^{204}Pb/^{206}Pb$ ratio.
4. For % Conc., 100% denotes a concordant analysis.
4. For % Conc., 100% denotes a concordant analysis
   following Tera and Wasserburg (1972) as outlined in Compston et al. (1991).

5. Discussion

The basement to the Katangan Sequence in the Lufilian Arc is only exposed in the Zambian Copperbelt. The sequence thickens significantly towards the Katanga Province of the DRC (Demesmaeker et al., 1963), where it is largely allochthonous and has been transported northwards along well defined nappe structures (Jackson et al., 2003). The nature of the basement over the entire 700 km extent of the Lufilian Arc can nevertheless be gauged using a combination of igneous crystallization and xenocrystic zircon ages. The following sections discuss the main features of the Palaeoproterozoic basement and attempt to place the new data from this study into a regional tectonic context.

a. Magmatic activity

Data obtained during this study shed light on the evolution of the Copperbelt basement. The petrography, and geochemistry of the Lufubu schists, located in four different areas of the Copperbelt, complemented by analyses taken from the literature, reveal that the precursors of the Lufubu schists are mainly volcanic in origin. Compositions range from andesite, rhyodacite-dacite to trachyandesite and alkali basalt, and analyses plot in the calc-alkaline field on an AFM diagram. Samples of Lufubu schists from this study also demonstrate a wide range of textures and compositions. In contrast, rocks from the Muva sequence in the Copperbelt are exclusively sedimentary in origin (Garlick, 1961b). Chemical analyses from the host rocks of the Samba Cu prospect suggest that they are volcanic in origin, and U-Pb zircon geochronology shows these rocks are of Palaeoproterozoic age. They must therefore be reclassified as Lufubu schist metavolcanics, and are not part of the Muva Supergroup [as previously regarded by Garrard (1965,1996) and Wakefield (1978)]. This study shows that the ages of the four samples of Lufubu schist from Chambishi (Zambia), Mufulira (Zambia), Samba (Zambia) and Kinsenda (DRC) span a period of ~106 Ma (1980 ± 7 Ma, 1968.1 ± 9.3 Ma, 1964 ± 12 Ma and 1873.5 ± 8.3 Ma respectively). Granitoids and granitoid gneisses, likewise, yield ages ranging from 2048.8 ± 5.8 Ma (Mkushi) to 1976.2 ± 4.8 Ma (Mulungushi) with intermediate events evident at 1993.7 ± 7.1 Ma (Mufulira) and at 1983 ± 5 Ma (Chambishi). The Lufubu schists record episodicity in the magmatic activity. Furthermore, the ages of the Lufubu schists together with the granitoids show that this magmatic activity was long lived, spanning nearly 200 Ma, and was represented by both intrusive and extrusive phases. This is best illustrated from the Chambishi basin where error bars on the ages of the Lufubu schists and the intrusive Chambishi Granite overlap. A plausible regional interpretation of these Palaeoproterozoic calc-alkaline terrains is that they were formed in a long-lived magmatic arc or series of arcs as a result of the subduction of oceanic lithosphere between 2.1 and 1.8 Ga. We suggest the name "Lufubu Metamorphic Complex" for this extensive, deformed and metamorphosed Palaeoproterozoic magmatic arc terrane in the Copperbelt basement.

b. Links with other Palaeoproterozoic terrains in the vicinity of the Congo Craton, and regional tectonic history

The Lufubu Metamorphic Complex of the Copperbelt basement, consisting of the Lufubu schist metavolcanics and associated plutonic granitoids, is continuous to the north with the Bangweulu Block (Ngoyi et al., 1991) (Figures 1 and 19). The granitoids and metavolcanics in the Bangweulu Block range in age from 1869 ± 20 to 1695 ± 43 Ma (Brewer et al., 1979; Schandelmeier et al., 1981, 1983; Kabengele et al., 1990; see above). This range encompasses part of the age range obtained from the Lufubu Metamorphic Complex in this study (2049-1874 Ma). If we include the 1750 ± 50 Ma age of the Roan Antelope Granite (Cahen et al., 1970c; see above), then the younger limits of the age ranges from both areas are comparable, whereas the Lufubu Metamorphic Complex has ages as old as ~ 2050 Ma, ~ 180 Ma older than the oldest dated rocks from the Bangweulu Block. However, it should be noted that all ages from the Bangweulu Block are Rb-Sr whole-rock isochrons, which may not reflect the intrusive ages, and instead may record a younger overprint or post-emplacement cooling. Such a situation is clearly exhibited by the Mkushi Gneiss, which has a U-Pb age of 2049 ± 6 Ma (this study), and a Rb-Sr whole-rock age of 1777 ± 89 Ma (Ng'ambi et al., 1986). The calc-alkaline magmatic rocks of the Lufubu Metamorphic Complex show certain petrographical and geochemical similarities to the granitoids and porphyritic metavolcanic rocks of the Luapula Porphyries of the Bangweulu Block in northern Zambia (Abraham, 1959; Thieme, 1970, 1971), and the Moba, Pepa-Lubumba and Lumono complexes of the Marungu Plateau, DRC (Tshimanga and Lubala, 1990; Kabengele et al., 1990, 1991). Minor quartzite and schist interbeds within the Marungu metavolcanics (Buttgenbach, 1905) may be the equivalents of similar metasedimentary rocks interbedded with the Lufubu metavolcanic rocks in the Lufubu Metamorphic Complex (e.g., Mendelsohn, 1961b).

To the west of the Copperbelt, the pre-Katangan basement rocks are exposed in several inliers in the Domes area of NW Zambia (Thieme and Johnson, 1981). Very imprecise dating of basement gneisses from the Mwombezhi dome has shown that the protoliths had ages of ca. 1.7 Ga, but were overprinted at ca. 1.2 Ga during the Irumide orogeny (Cosi et al., 1992). In the Kabompo Dome of NW Zambia, the major pre-Katangan lithologies are biotite gneisses, augen gneisses, migmatites, foliated granites, feldspar-phyric biotite granite, mica schists and pegmatites (Klinck, 1977; Liyungu and Njamu, 2000). Feldspar-phyric granites from the Kabompo Dome have yielded SHRIMP zircon U-Pb ages of 1940 ± 2.8 Ma and 1934 ± 6 Ma (Key et al., 2001). In the Kalumbila Co-Ni-Cu deposit, detrital zircons from the Katangan metasedimentary host rocks have yielded SHRIMP U-Pb ages between 2004 and 1884 Ma, interpreted to reflect derivation from the Palaeoproterozoic granitic gneisses exposed in the adjacent Kabompo Dome

(Steven and Armstrong, 2003). In the Mwinilunga area of NW Zambia, near the borders with Angola and the DRC, Key et al. (2001), have obtained a SHRIMP U-Pb zircon age of 2058 ± 7 Ma for a porphyritic granite. This age is within error of the age of the Mkushi gneiss (2049 ± 6 Ma) obtained in this paper. The age range of the basement rocks in the Domes and Mwinilunga areas of NW Zambia, as well as their lithological make up, thus indicates a strong similarity with the rocks of the Kafue anticline in the Copperbelt area, and with the granites and gneisses of the Mkushi-Mulungushi area, which collectively belong to the Lufubu Metamorphic Complex. Recently a granitic gneiss near Kapiri Mposhi yielded a U-Pb zircon emplacement age of 2.73 Ga (de Waele and Fitzsimons, 2004). This gneiss, which is situated between the Kafue anticline and the Mulungushi gneiss, is here interpreted as a sliver of an exotic terrane within the Palaeoproterozoic arcs of the Lufubu Metamorphic Complex.

Farther west and southwest of the Kabompo Dome and Mwinilunga areas of Zambia, the Katangan rocks and their basement are buried under Phanerozoic Karoo and Kalahari sand cover of the Kalahari basin (Money, 1972; Thieme and Johnson, 1981). Interpretations of regional gravity and airborne magnetic surveys of western Zambia have shown that the structural trends of the basement rocks of western Zambia strike NE-SW, along a southwesterly prolongation of the trend of the western part of the Lufilian Arc (Saviaro, 1978, 1979). Gravity maps of NW Botswana (Reeves, 1978; McMullan et al., 1995) and airborne magnetic maps of Botswana and Namibia (Reeves, 1979; Eberle et al., 1996) show the smooth continuation of the Lufilian geophysical trends of western Zambia into the Damaran belt of NW Botswana and northern Namibia, with no significant breaks. This implies a continuity of the basement terranes between Zambia and Namibia. In northwestern Botswana, the Quangwadum augen gneiss, from a basement inlier west of the Okavango delta, was recently dated at ~ 2050 Ma with the U-Pb technique on single zircons (Singletary et al., 2003). Further west, in NE Namibia, in the Tsumkwe inlier close to the Botswana border, Hoal et al.

(2000) obtained a SHRIMP U-Pb zircon age of 2022 ± 15 Ma from a fine-grained granitic gneiss. This age is not only similar to that of the Quangwadum gneiss, but is also comparable to the ages of the Mwinilunga porphyritic granite and the Mkushi Gneiss from Zambia. Also in the Tsumkwe area, Hoal et al. (2000) have obtained a SHRIMP U-Pb zircon age of 852 ± 11 Ma for a megacrystic granite. This date falls within the age range defined by the Nchanga granite (877 ± 10; Armstrong et al., 1999, 2004) and the Lusaka granite (842 ± 33 Ma; recalculated from the data of Barr et al., 1977).

In northern Namibia, west of the Tsumkwe area, the pre-Damaran basement, consisting of various granitoids, the Huab gneisses, and the volcanosedimentary Khoabendus Group, is exposed in the Grootfontein, Kamanjab and Huab inliers (Clifford et al. 1962; Frets, 1969; Guj, 1970; Porada, 1974). Limited age dating in the Kamanjab inlier (also known as the Franzfontein inlier) has revealed the existence of a Palaeoproterozoic magmatic arc terrane having ages between ~ 1987 Ma and ~ 1662 Ma (Burger et al., 1976; Tegtmeyer and Kröner, 1985). Recently, a rhyolitic quartz porphyry of the Khoabendus Group in the Kamanjab inlier, has been dated at 1862 ± 6 Ma (Steven and Armstrong, 2002). In NW Namibia, the granitic augen gneiss of Ruacuna was dated at 1795 +33/-29 Ma with the U-Pb technique on multigrain zircon fractions (Tegtmeyer and Kröner, 1985). In the Central Zone of the Damara belt, north of the suture with the Kalahari craton, pre-Damaran basement of the southernmost Congo Craton is exposed in the Abbabis inlier and in various smaller gneissic exposures (Jacob et al., 1978). Zircon fractions from the basement gneisses have yielded U-Pb concordia upper-intercept ages of 1925 +330/-280 Ma and 1945 ± 18 Ma, from the Abbabis Inlier and the Tumas Dome, respectively (Jacob et al., 1978; Burger and Jacob, unpublished data, in Kröner et al., 1991). Tack et al. (2002) obtained a SHRIMP U-Pb zircon age of 2038 ± 5 Ma from augen gneiss in the Ida Dome, and they also found ca. 2050 Ma xenocrystic zircon cores occurring in ca. 542 Ma Damaran granitoids. In the Khan Gorge near the Rössing uranium mine, Kröner et al. (1991) found xenocrystic zircon grains with ages of 2014 ± 39 Ma and 2093 ± 51 Ma from c. 1038 Ma and 1102 Ma granitoid gneisses, respectively. These various studies indicate that the pre-Damara basement of the southern Congo Craton is mainly Palaeoproterozoic, together with some late Mesoproterozoic components (Kröner et al., 1991), which are similar to those from the Irumide Belt. The age range of the Palaeoproterozoic basement, between 2093 ± 51 Ma and 1925 +330/-280 Ma, is similar to that of the basement inliers of northern Namibia and NW Botswana. As was pointed out by Master (1990, 1993), all these terrains may form a continuum with the Domes area of NW Zambia, the Lufubu Metamorphic Complex of the Central African Copperbelt basement, and the Bangweulu Block and define a Palaeoproterozoic magmatic arc along the S and SE margin of the Congo Craton. We refer to this magmatic arc as the Kamanjab–Bangweulu terrane.

The NW-SE trending Ubendian Belt, which separates the Bangweulu Block from the Archaean Tanzanian craton (2.93-2.53 Ga in age; Pinna et al., 1996, 1999), is an orogenic belt dated at between ca. 2.0 and 1.85 Ga (Schandelmeier, 1983; Lenoir et al., 1994; Boven et al., 1999). It consists of strongly sheared amphibolite-facies quartzofeldspathic ortho- and paragneisses, amphibolites, anorthosites, and granitoids, with subvertical foliations, which are found in several discrete fault-bounded terranes (Daly, 1988; Ring et al., 1997). The Ubendian Belt may be the result of the collision of the Kamanjab-Bangweulu magmatic arc terrane, or at least the Bangweulu Block, and the Tanzanian craton. This collision occurred between 2.0 and 1.9 Ga ago (Ring et al., 1997), and resulted in a foliation in Bangweulu Block granitoids. This was followed by the intrusion of post-tectonic granites, which are dated at 1869 ± 20 Ma, 1838 ± 43 Ma and 1824 ± 75 Ma (Schandelmeier, 1981, 1983). The sedimentary Mporokoso Group unconformably overlies these granitoids, hence there is possibly no connection between it and the Mpanshya River Group in the Irumide Belt (which was deposited at 1880 ± 12 Ma), even though they were correlated by Daly and Unrug (1982) and de Waele and Mapani (2002). After being sutured in the Ubendian Belt, the Kamanjab-Bangweulu terrane and Tanzanian craton formed a single unified minicontinent, the “Kambantan” terrane (named acronymically after its component parts), which eventually was accreted onto the Kasai-Angola Block to form the southeastern and southern part of the enlarged Congo Craton. The Ubendian belt suffered major re-activation during later Irumide and Pan-African tectonism (Daly, 1986; Theunissen et al., 1992).

In Zambia and the DRC, the Bangweulu Block is separated from the Archaean to Palaeoproterozoic (2.9-2.2 Ga; Delhal and Ledent, 1973; Delhal et al., 1976; Bassot et al., 1981) Kasai-Angola Block by the Mesoproterozoic (ca 1.4-1.0 Ga) Kibaran belt. The Kibaran belt, which consists of a thick pile of quartzitic and pelitic metasedimentary rocks and gneisses, together with intrusive granitoids, records a cycle of sedimentation followed by magmatic intrusion, collisional deformation and metamorphism, and post-tectonic granitic intrusion (Cahen et al., 1984). Earlier notions of an intracontinental rift setting for the Kibaran Belt (Klerkx et al., 1987) have now been superceded by evidence supporting the operation of a full Wilson cycle, involving rifting, ocean opening and closure, followed by subduction and collision (Kampunzu et al., 1986; Rumvegeri, 1989, 1991; Kokonyangi et al., 2002). Burke (2003) has shown that the Kabanga-Musongati Line of mafic-ultramafic complexes, that separates the Eastern External and the Western Internal Domains of the NE Kibaran Belt (Tack et al., 1994), likely represents the deeply eroded roots of an Andean-type magmatic arc. Whereas the NE Kibaran Belt of Rwanda and Burundi is over 200 km wide, it tapers wedge-like to the SW into the DRC, and then disappears completely in the Mwinilunga area of NW Zambia, where recent mapping by Key et al. (2001) has shown that only Archaean and Palaeoproterozoic rocks are present, with numerous NE-SW trending ductile shears and brittle fractures being the only representatives of possible Kibaran structures in this area. Farther west, these structures, together with all other basement rocks, are obscured by sedimentary cover of the Kalahari Basin of eastern Angola, for which no subsurface geophysical or borehole information is available. However, the southwestern continuation of the Kibaran trends can be followed to SW Angola, where the basement rocks emerge again. Here there is evidence that the Palaeoproterozoic rocks that characterise much of the Precambrian of southern Angola (Bassot et al., 1981; Carvalho et al., 2000; McCourt et al., 2004), have been overprinted during the Kibaran Orogeny (Carvalho et al., 1987). The Cunene Anorthosite Complex, which is regarded as a Grenvillian-type massif anorthosite (Ashwal and Twist, 1994), has recently been assigned Kibaran ages of 1370 ± 4 Ma and 1385.0 ± 7.6 Ma (Morais et al., 2000; Mayer et al., 2000; McCourt et al., 2004), based on zircon U-Pb ages of a crosscutting co-genetic mangerite dyke.

Recent metamorphic and geochronological work in the Epupa gneisses south of the Kunene Anorthosite Complex has revealed the existence of two orogenic events here- a Kibaran event at ca. 1.3 Ga (Seth et al., 2001), and an earlier event, in the Epembe granulites, at ca. 1.5 Ga, which has not been recorded before in Central Africa (Seth et al., 2003). A hint at the existence of a more widespread ca. 1.5 Ga event in Central Africa is given by the presence of xenocrystic zircons dated at ca. 1.5 Ga in a Katangan lapilli tuff in the DRC (Rainaud et al., 2003). The ca. 1.5 Ga "Epembe" event, which involved burial of post-1.63 Ga metapelites to the lower crust followed by rapid exhumation (Brandt et al., 2003), was probably a short lived event, being a record of a brief encounter between the southern Kasai-Angola block and an unknown terrane, speculated by Seth et al., 2003, to be possibly one of the few ca. 1.5 Ga terranes known worldwide, i.e., Rondonia (Brazil), the Pinwarian (Grenville Province, Canada) or the Gothian (Baltic Shield, Sweden). The ca. 1.5 Ga event was then followed by the Kibaran cycle, between 1.4 and 1.0 Ga, which is represented in this area by the Orue gneisses, dated at 1334 ± 21 Ma, and red granites from southern Angola (1411-1302 Ma, Rb-Sr ages; Bassot et al., 1981; Seth et al., 2001, 2003)

In order to explain the apparent southwestwards disappearance of the Kibaran Belt in NW Zambia, and its re-appearance in SW Angola and NW

Nambia, we propose that the Kibaran Belt has been overthrust by the Kambantan minicontinent when this terrane collided with the Kasai-Angola Block during the Kibaran Orogeny. Hence the apparent southwestwards wedging out of the Kibaran belt is explained by progressive overthrusting by the Kambantan terrane late in the Kibaran orogeny. This model is illustrated schematically in Figure 30. Section A-A' shows a section from the Kasai-Angola Block to the Bangweulu Block, north of the Lufilian Arc. Here the Kibaran metasedimentary rocks (part of which formed a passive margin to the Kasai-Angola Block) are shown as a deformed belt between the Kasai-Angola Block and the Kambantan terrane. Forming the cover of the Kambantan terrane, is the Mporokoso Group, overlain by the tabular Katangan sequence. In Section B-B', which runs parallel to the first section, but further south, passing through the Mwinilunga area of NW Zambia and the Lufilian Arc, the contact between the Kasai-Angola Block and the Kambantan terrane is a major thrust (corresponding to the NE-SW trending ductile shear zones with down-dip lineations mapped by Key et al., 2001), which has over-ridden, at depth, the deformed Kibaran metasedimentary belt together with its intrusive granitoids. Forming a cover to the Kambantan terrane in this section are the Muva Group and the tectonically thickened pile of Katangan sediments. Also shown on this section is the 3.2-3.0 Ga Likasi terrane, which is a cryptic terrane whose existence was revealed by the presence of Mesoarchaean xenocrystic zircons in Katangan lapilli tuffs from the central Lufilian Arc (Rainaud et al., 2003). In the Mwinilunga area, Key and Armstrong (2000) showed that zircons from 2540 Ma granites of the Kasai-Angola Block contained xenocrystic cores with ages up to 3154 Ma, interpreted by Rainaud et al. (2003) as being derived from the underlying Likasi terrane. Our section shows the inferred contact between the 2.8-2.4 Ga high-grade (granulite facies) gneisses of the Kasai-Angola Block, and the Mesoarchaean Likasi cryptic terrane, which underlies the Neoarchaean (2.54-2.53 Ga) granitic gneisses dated by Key et al. (2001), as well as the Kibaran Belt. The post-Muva, pre-Katangan plutonism of the Nchanga granite is also indicated on the section. A late Kibaran age for the major thrust

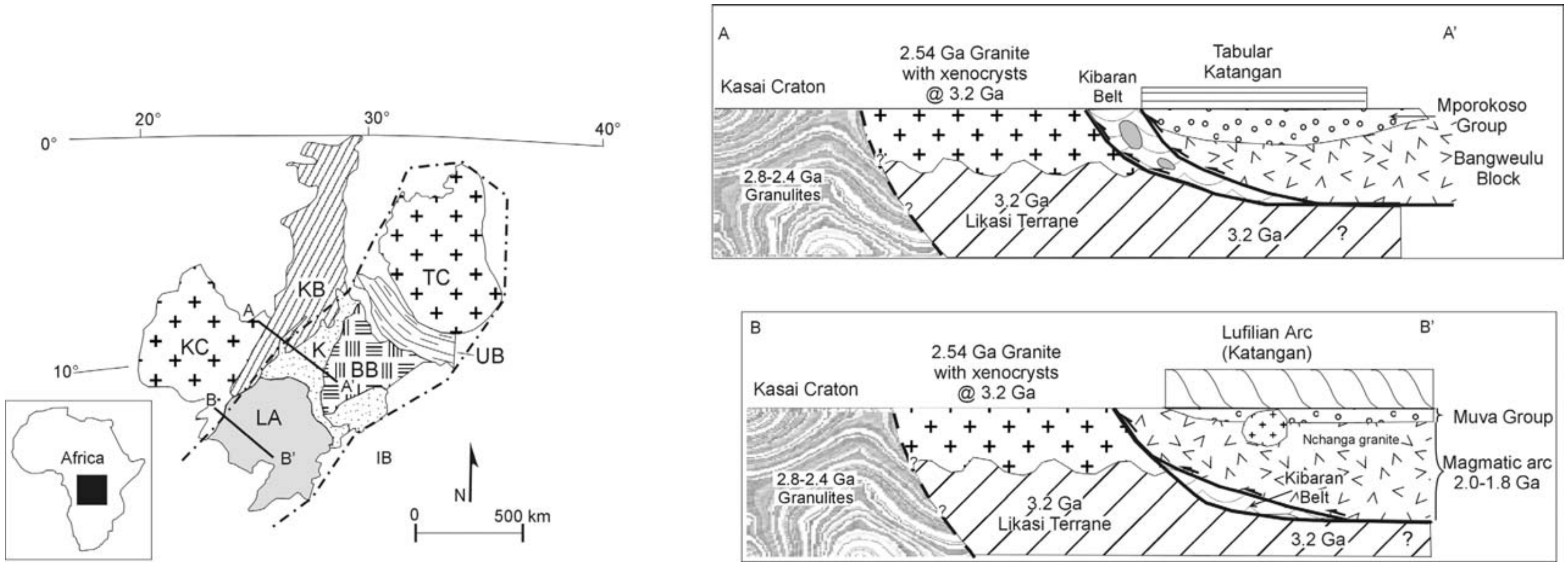

Figure 30: Sketch map of central Africa showing the major lithostructural units and two cross sections A-A' and B-B' discussed in the text. BB – Bangweulu Block; IB – Irumide Belt; K – Kundelungu Plateau; KB – Kibaran Belt; KC – Kasai Craton; LA – Lufilian Arc; TC – Tanzanian Craton; UB – Ubendian Belt. Dashed and dotted line indicated the outline of the northeast portion of the Kambantan Terrane.

underlying the Kambantan terrane is constrained by the presence of a population of xenocrystic Kibaran-aged zircons (1273 ± 46 to 1018 ± 27 Ma) located in the same pyroclastic layer from the Katangan sequence that contains the Mesoarchaean zircons from the Likasi terrane (Rainaud et al., 2003). If the thrusting of the Kambantan terrane over the Kibaran belt occurred later, during the Pan-African Lufilian orogeny (which post-dated the deposition of the Katanga Supergroup), then no Kibaran-aged xenocrystic zircons would have been present in the Katangan tuffs.

Following the accretion of the Kambantan terrane onto the southern part of the Congo craton during the Kibaran orogeny, another series of terranes collided outboard of this, to produce the Irumide belt, whose metamorphic peak was at ca. 1050 to 1020 Ma (Schenk and Appel, 2001, 2002; de Waele et al., 2003). Irumide-aged gneisses (Kröner et al., 1991, see above) and metavolcanics (Steven et al., 2000) are also found in inliers of the southern Congo craton within the central Damara Belt of Namibia and in NW Botswana (Kampunzu et al., 1998; Singletary et al., 2003), indicating that the Irumide orogeny was more extensively developed on the southern margin of the Congo craton. The Irumide terranes include supra-subduction zone magmatic rocks and small Archaean microcontinental slivers dated at c. 2.6 Ga (Johnson and Rivers, 2004; Johnson et al., 2004; Mapani et al., 2004). The lack of syn-collision-related granitoid magmatism, together with the high temperature-low pressure metamorphism, suggests that the Irumide belt formed in an active Andean or Cordilleran type setting (Johnson and Rivers, 2004; Johnson et al., 2004). Many of these Irumide terranes in the southern part of the Congo craton (north of the Mwembeshi dislocation zone) rifted away during the opening of the Khomas ocean at c. 750-730 Ma (Hoffman, 1994), to form a rifted passive margin of the Congo craton, in which Damaran and Katangan sediments were deposited.

During the Pan-African Damaran-Lufilian orogeny, the Khomas ocean closed with subduction of oceanic lithosphere underneath the Congo craton margin, leading to the formation of an Andean-type magmatic arc, and ultimately to the Himalayan-type collision between the Congo and Kalahari cratons at about 550-510 Ma (Miller, 1983; Porada and Berhorst, 2000). Eclogites and talc-kyanite whiteschists formed during the collision record extremely high pressures, compatible with a closure of an ocean at least 1000 km wide (John et al., 2003). Thus models for the formation of the Damara-Lufilian-Zambezi orogen due to the collision of the Congo and Kalahari cratons (Burke et al., 1973) are being vindicated, at the expense of models which regard the Katangan-Damaran sequences as having formed in interlinked intracontinental rifts or narrow ocean basins (e.g., Hanson et al., 1994; Hanson, 2003). One of the reasons why Hanson (2003) supported the intracontinental rift model was the apparent continuity of the Irumide belt into the Choma-Kalomo belt, across the Neoproterozoic Zambezi Belt. Recent age dating has shown that the Irumide and Choma-Kalomo belts have dissimilar ages, differing by up to 200 Ma, and that postulates of their former continuity are invalid (de Waele et al., 2003; Johnson and Rivers, 2004). Hence, earlier models which attempted to link the Palaeoproterozoic basement of the Central African Copperbelt with terranes that are now a part of the Kalahari craton, (such as a magmatic arc extending to the Richtersveld region of southern Namibia, with the Kheis and Magondi belts being back-arc basins to this arc; Master, 1990, 1993), are now regarded as being invalid.

In NW Namibia, the N-S trending Kaoko belt marks the site of a transpressive collision between the Congo craton and the Rio de la Plata craton of South America (Dürr and Dingledey, 1996; Goscombe et al., 2003), and it may have preceded the closure of the Khomas sea in the NE-trending Damara Belt (Prave, 1996). U-Pb zircon age dating has revealed the presence of Palaeoproterozoic (ca. 1978-1933 Ma) basement rocks within this belt, as well as rocks which are as old as 2645-2585 Ma (Seth et al., 1998), and as young as 1.53-1.50 Ga (Kröner et al., 2002). The Archaean ages from this belt are regarded as coming from rocks that are part of an accreted exotic terrane that originated probably in the Rio de la Plata Craton and was left behind in Africa after the opening of the Atlantic Ocean. The Palaeoproterozoic ages probably reflect the age of the Kamanjab-Bangweulu terrane, which formed the basement as well as the foreland of the Kaoko orogeny.

c. Inherited zircons

Five samples in our study showed signs of inheritance of older zircons. The sample LufMuf, a Lufubu schist from Mufulira, showed four zircon ages which are older than the 1968 ± 9 Ma emplacement age of the Lufubu schists. One zircon yielded a $^{207}Pb/^{206}Pb$ age of 2174 ± 13 Ma and the three remaining zircons yielded a weighted mean $^{207}Pb/^{206}Pb$ age of 2057 ± 9 Ma. The oldest zircon reveals the presence of crustal components as old as 2.17 Ga, while the three younger zircons have an age comparable to that of the Mkushi Gneiss, indicating that rocks of the age of the Mkushi Gneiss precursor were more widespread, and formed part of the source region, or were in the path of ascent, of the magmas that produced the precursor volcanic rocks of the Lufubu schists.

The cores of zircons from the Mtuga aplite sample APL-1, from the Mkushi Mine, yielded a range of $^{207}Pb/^{206}Pb$ ages between 2072 ± 9 Ma and 2009 ± 4 Ma. Zircons from Mtuga aplite sample APL-2 have inherited cores that range in age mainly from 2064 ± 15 to 1998 ± 18 Ma, with two older ages of 2730 ± 7 and 2688 ± 8 Ma. The age range of the zircon cores from the two aplites encompasses the age of the 2049 Ma Mkushi Gneiss, as well as the 2050-2020 Ma range of detrital zircon core ages from the Serenje paragneisses and migmatites north of Mkushi (de Waele and Mapani, 2002). Hence, the zircon cores from the Mtuga aplites are interpreted as being xenocrystic and may be inherited from a protolith similar to the Serenje gneisses and migmatites, which underwent partial melting. Omenetto (1973, 1974) had argued earlier that the mineralized aplites from the Mkushi area were derived from "granitization", regarded as the time as melting, of a sedimentary paragneiss precursor which contained disseminated Cu mineralization which was partitioned into the granitic melt.

The two Neoarchaean zircon cores from APL-2, at 2730 ± 7 Ma and 2688 ± 8 Ma, are the only Archaean xenocrysts found in any of the basement granitoids. If, as argued above, the aplites are derived from partial melting of a metasedimentary paragneiss precursor, then the Archaean zircons would have to have been part of the detrital zircon population in the metasediment. The two Archaean zircon core ages are also similar to the ages of detrital monazites found in Irumide quartzites from the Irumi Hills (near Mkushi), and the Changwena Hill (SW of Serenje), which have respectively been dated at 2720 ± 24 Ma and 2720 ± 20 Ma (Snelling et al., 1964). The source of these Archaean detrital zircons and monazites is likely to be the newly discovered gneisses at Kampoya quarry, some 40 km northwest of Mkushi Mine, which have been dated at 2.73 Ga (de Waele and Fitzsimons, 2004). The ages of detrital zircons and monazites in the Irumide Belt also corresponds with the ages of detrital zircons found in the Muva quartzite south of Mufulira in the Copperbelt, which range from 1991 to 3180 Ma, including a cluster of ages between 2708 ± 18 and 2463 ± 25 Ma (Rainaud et al., 2003). However, Mesoarchaean zircons dated between 3.2 to 3.0 Ga, which are present in the Muva quartzites near Mufulira, are absent from the detrital population in quartzites and paragneisses in the Irumide belt (De Waele and Fitzsimons, 2004), as well as in the xenocrystic zircon population in aplites derived by partial melting of the Irumide metasediments. This suggests that the detrital zircon populations in the Muva quartzites have a different origin from those in the Irumide quartzites and paragneisses. The Muva quartzites of the Copperbelt include detrital components from the Mesoarchaean Likasi terrane of the southern Congo craton (Rainaud et al., 2003), and could only have been deposited after the amalgamation of the Kambantan terrane with the Congo craton during the Kibaran orogeny. Thus, despite containing no detrital zircons younger than 1941 Ma (Rainaud et al., 2003), the Muva in the

Copperbelt may represent some kind of post-orogenic molasse deposit following the Kibaran orogeny.

Sample CT169/1256, from the Samba prospect, yielded three inherited zircons dated at 2423 ± 13, 2336 ± 9 and 2160 ± 25 Ma respectively. The youngest of these xenocrystic zircons (2160 ± 25 Ma) has an age similar to the oldest xenocryst from Mufulira, dated at 2174 ± 13 Ma, and is likely to be derived from a similar source. The two older xenocrysts from Samba indicate the presence of crustal components as old as 2.42-2.33 Ga in the source region, or in the path of ascent, of the magmas that produced the precursor volcanic rocks to the Samba Lufubu schists.

Fine pyroclastic layers from the Neoproterozoic Katangan sequence (sample Etoile 1) yielded two Mesoarchaean zircons at 2831 ± 16 Ma and 2802 ± 36 Ma and one Palaeoproterozoic zircon at 1858 ± 24 Ma. As is the case for Archaean zircons in tuffs from the overlying Mwashya Group, the two Archaean zircons from the Etoile 1 tuff sample may be derived from cryptic Archaean terranes which have been tectonically overridden by the Lufilian arc, such as the Likasi terrane, or other portions of the Congo Craton (Rainaud et al., 2003). Ages of ca. 2.8 Ga have been found in the southern exposed part of the Congo Craton in the Kasai region (Delhal et al., 1976). A xenocrystic zircon dated at 2839 ± 22 Ma was reported from a foliated Archaean granite in the Mwinilunga area of NW Zambia, which had an intrusive age of 2538 ± 10 Ma (Key et al., 2001). The third zircon, in the Etoile 1 sample, with an age of 1858 Ma, is clearly derived from the Palaeo-proterozoic basement of the Copperbelt, the Lufubu Metamorphic Complex.

Inherited zircons from the Samba porphyry and Mufulira Lufubu schists may derive from cryptic terranes ranging in age from 2400 Ma to 2100 Ma. No rocks of such an age have yet been dated from the Copperbelt basement. Finally, no sample of the Lufubu schists or the Palaeoproterozoic granitoids has yielded xenocrystic zircons with Archaean ages. This suggests that the protoliths of the Lufubu Metamorphic Complex developed as juvenile crust far from older continental influences, in an oceanic island arc environment rather than in an Andean-type arc.

Nd and Pb isotopic studies of Damaran metasedimentary and granitoid rocks by Hawkesworth et al. (1981) and Hawkesworth and Marlow (1983) indicate these rocks were derived from basement rocks up to 2 Ga in age, and suggest an absence of any significantly older crust beneath the Damara Orogen. However, just as the detrital zircons from the Muva cover rocks of the Lufubu Metamorphic Complex have much older ages, indicating partial derivation from an Archaean terrane (Rainaud et al., 2003), so also do detrital zircons from Damaran cover rocks have much older ages than their immediate basement. Jacob et al. (2000) have dated detrital zircons from the Damaran metasediments that host the Navachab gold deposit in the Karibib District, and have obtained SHRIMP U-Pb ages of 2872 ± 4 Ma, 2870 ± 6 Ma, 2428 ± 9 Ma, 2360 ± 5 Ma, and 1962 ± 10 Ma. The ca. 2.8-2.4 Ga ages are similar to ages obtained from the Congo Craton in Kasai, DRC (Delhal and Ledent, 1973; Delhal et al., 1976), and they also encompass the age range of xenocrystic zircons from the Samba metavolcanics and the Katangan pyroclastics from the Copperbelt (see above). This may suggest that by the time the Neoproterozoic Katangan and Damaran sedimentation occurred, the Kambantan terrane had already been sutured to the Archaean Kasai-Angola block, from which detrital components were shed into cover sequences on the younger terrane. Although no Archaean detrital zircons have yet been found in the Katanga Supergroup (Master et al., 2004), detrital platinoids in Katangan sediments at Mutoshi in the Kolwezi area have been inferred to be derived from the Archaean Kasai-Angola Block (Jedwab, 1997). In these same Katangan sediments, Jedwab (1997) also reported detrital cassiterite grains which were probably derived from erosion of late Kibaran tin-granites.

6. Conclusions

The basement to the Katangan Supergroup in the Central African Copperbelt consists of the Lufubu schists and various granitoids and gneisses, which constitute the newly defined Lufubu Metamorphic Complex. The Lufubu schists represent a long-lived calc-alkaline volcanic arc sequence and, where dated in both Zambia and the Democratic Republic of Congo (DRC), yield ages of 1980 ± 7, 1968 ± 9, 1964 ± 12 and 1874 ± 8 Ma. The Mkushi granitic Gneiss from south-east of the Zambian Copperbelt, has an age of 2049 ± 6 Ma. An augen gneiss, from the Mulungushi Bridge locality, yielded an emplacement age of 1976 ± 5 Ma. More evolved granitoids from the Copperbelt itself, the Mufulira Pink Granite and the Chambishi Granite, gave ages of 1994 ± 7 and 1983 ± 5 Ma respectively. These gneisses, granitoids and acid-intermediate calc-alkaline metavolcanics are considered to represent stages in the evolution of a magmatic arc or several arcs that formed episodically over a 200 million year period between 2050 and 1850 Ma. The undeformed, copper-mineralized Mtuga aplites, which crosscut the foliation in the Mkushi gneisses, have xenocrystic cores similar in age to the gneisses, with overgrowths dated at 1059 ± 26 Ma, regarded as the age of igneous emplacement of these aplites, which thus intruded during the Irumide orogeny.

We interpret the rocks of the Lufubu Metamorphic Complex as belonging to a regionally extensive Palaeoproterozoic magmatic arc terrane stretching from northern Namibia to northern Zambia and the Marungu Plateau of the DRC, the Kamanjab-Bangweulu terrane, which collided with the Archaean Tanzanian craton during the ca. 2.0-1.9 Ga Ubendian orogeny, to produce a new composite minicontinental entity that we term the “Kambantan” terrane. The Kambantan terrane was accreted onto the southern margin of the Congo Craton during the Mesoproterozoic ca. 1.4-1.0 Ga Kibaran orogeny. The outboard side of the Kambantan terrane was the site of the ca. 1.05-1.02 Ga Irumide orogeny, caused by the collision of several terranes with the Congo craton. Part of the Irumide belt subsequently rifted off at ca. 750-730 Ma, leading to the formation of a rifted passive margin during sedimentation of the Damara and Katanga Supergroups, and the opening of an ocean basin which closed during the Pan-African Damaran-Lufilian orogeny, when the Congo and Kalahari cratons were sutured together.

ACKNOWLEDGEMENTS

This paper is dedicated to the memory of Patrick Mumba (1956-2001) who initiated this study of the Palaeoproterozoic basement of the Copperbelt, and who collected some of the samples from Mkushi, Mufulira and Mulungushi Bridge. We are indebted to Anglovaal Limited for funding this study and for permission to publish the results. We are grateful for the help received from Claus Schlegel of Anglovaal Zambia; Mufulira Copper Mine, Zambia; Kinsenda Mine, DRC; the late Chad Kaunda from ZCCM in Kalulushi; and Flungu Musendu in the DRC. Samples from Baluba were collected by SM during the IGCP 363 Field Meeting in 1996. SM is also deeply indebted to Kevin Burke for insightful discussions on the Kibaran and Irumide orogenies, and on global tectonics. We thank Richard Hanson for his careful and insightful review, which has considerably improved this paper.

7. References

Abraham, D., 1959. *The stratigraphical and structural relationship of the Kundelungu System, Plateau Series and basement rocks in the Mid-Luapula valley, Northern Rhodesia*. D. Phil. Thesis, University of Leeds, 152 pp.

Ackermann, E., 1935. Migmatite im Kristallin der Rhodesischen Masse. Geologische Rundschau, 26, 454-455.

Ackermann, E., 1936. Das Problem der Mkushigneise am NW-Rand der Rhodesischen Masse. Geologische Rundschau, 27, 81-87.

Andersen, L. S., Unrug, R., 1984. Geodynamic evolution of the Bangweulu Block, northern Zambia. *Precambrian Research*, **25**, 187-212.

Armstrong, R.A., Robb, L.J., Master, S., Kruger, F.J., Mumba, P.A.C.C., 1999. New U-Pb age constraints on the Katangan Sequence, Central African Copperbelt. In: Frimmel, H.E. (Ed.), Special Abstracts Issue: 11th International Conference of the Geological Society of Africa: Earth Resources for Africa. J. Afr. Earth Sci., 28(4A), May 1999, 6-7.

Armstrong, R.A., Master, S., Robb, L.J., Lobo-Guerrero, A., 2004. Geochronology of the Nchanga Granite, and constraints on the maximum age of the Katanga Supergroup, Zambian Copperbelt. In: Robb, L.J., Sutton, S., Cailteux J. (Eds.), Special Issue on the Central African Copperbelt, Journal of African Earth Sciences.

Ashwal, L.D., Twist, D., 1994. The Kunene complex, Angola/Namibia: A composite massif-type anorthosite complex. Geological Magazine, 131(5), 579-591.

Auger, F., 1975. Manifestations volcaniques dans le Roan inférieur et dans la "Série des mines" du Shaba (République du Zaïre). Annales de la Faculté des Sciences, Géologie et Géographie, Université Nationale du Zaïre, Lubumbashi, 1, 35-42.

Bancroft, J.A., Pelletier, R.A., 1929. Notes on the general geology of Northern Rhodesia. 15th Int. Geol. Congr. Guide Book (Excursion C22), Pretoria, South Africa, 1-12.

Barr, M.W.C., Cahen, L., Ledent, D., 1977. Geochronology of syntectonic granites from central Zambia: Lusaka granite and granite NE of Rufunsa. Annales de la Société Géologique de Belgique, 100, 47-54.

Bassot, J.P., Pascal, M., Vialette, Y., 1981. Données nouvelles sur la stratigraphie, la géochimie et la géochronologie des formations précambriennes de la partie méridionale du Haut Plateau angolais. Bulletin du Bureau de Recherches Géologiques et Minières, Section 4, Géologie Générale 4, 285-309.

Boven, A., Theunissen, K., Sklyarov, E., Klerkx, J., Melnikov, A., Mruma, A., Punzalan, L., 1999. Timing of exhumation of a high–pressure mafic granulite terrane of the Paleoproterozoic Ubende belt (West Tanzania). Precambrian Research, 93, 119-137.

Brandt, R.T., Burton, C.C.J., Maree, S.C., Woakes, M.E., 1961. Mufulira. In: Mendelsohn, F. (Ed.), *The Geology of the Northern Rhodesian Copperbelt*. MacDonald, London, 411-461.

Brandt, S., Klemd, R., Okrusch, M., 2003. Ultrahigh temperature metamorphism and multistage evolution of garnet-orthopyrozene granulites from the Proterozoic Epupa Complex, NW Namibia. Journal of Petrology, 44, 1121-1144.

Brewer, M.S., Haslam, H.W., Darbyshire, D.P.F., Davis, A.E., 1979. Rb-Sr age determinations in the Bangweulu Block, Luapula Province, Zambia. Institute of Geological Sciences, London, Report 79/5, 1-11.

Brock, B.B., 1961. The structural setting of the Copperbelt. In: Mendelsohn, F. (Ed.), *The Geology of the Northern Rhodesian Copperbelt*. Macdonald, London, 81-89.

Burke, K., Dewey, J.F., Kidd, W.S.F., 1973. World distribution of sutures- the sites of former oceans. Tectonophysics, 40, 69-99.

Burke, K., 2003. Assembly of the Congo Craton at ca. 1 Ga. In: Burke, K.C.A., Dewey, J.F., Sengör, A.M.C. Plate Tectonics and Precambrian Geology. Short Course Notes, 3-5 September 2003, University of the Witwatersrand, Johannesburg, 22 pp.

Burger, A.J., Clifford, T.N., Miller, R.McG., 1976. Zircon U-Pb ages of the Franzfontein granitic suite, northern South West Africa. Precambrian Research, 3, 415-431.

Buttgenbach, H., 1905. Observations géologiques faites au Marungu (1904). Ann. Soc. Géol. Belg., 32 (1904-5), 315-327.

Cahen, L., Ledent, D., Pasteels, P., Delhal, J., Grögler, N., 1968. Détermination d'âge sur les granites anciens (anté-katangiens) et jeunes (Katangiens) du Copperbelt de Zambie et du Katanga Sud-Oriental (Note préliminaire). Ann. Soc. géol. Belg., 91, 313-315.

Cahen, L., Delhal, J., Ledent, D., 1970a. On the age and petrogenesis of the microcline-bearing pegmatite veins at Roan Antelope and at Musoshi (Copperbelt of Zambia and S-E Katanga). Ann. Mus. roy. Afr. Centr., Sci. géol., 65, 43-68.

Cahen, L., Delhal, J., Ledent, D., Pasteels, P., 1970b. Isotopic data relative to the age and petrogenesis of dome-forming granites in the Copperbelt of Zambia and S-E Katanga. Ann. Mus. Roy. Afr. Centr., Sci. géol., 65, 69-107.

Cahen, L., Delhal, J., Deutsch, S., Grögler, N., Pasteels, P., 1970c. The age of the Roan Antelope and Mufulira granites (Copperbelt of Zambia). Ann. Mus. Roy. Afr. Centr., Sci. géol., 65, 15-42.

Cahen, L., Snelling, N.J., 1966. *The Geochronology of Equatorial Africa*. North Holland, Amsterdam, 195 pp.

Cahen, L., Snelling, N.J., Delhal, J., Vail, J.R., Bonhomme, M., Ledent, D., 1984. *The Geochronology and Evolution of Africa*. Clarendon Press, Oxford, 512 pp.

Carvalho, H., Crasto, J.P., Silva, Z.C.G., Vialette, Y., 1987. The Kibaran cycle in Angola- a discussion. Geological Journal, 22, 85-102.

Carvalho, H., Tassinari, C., Alves, P.H., Guimarães, F., Simões, M.C., 2000. Geochronological review of the Precambrian in western Angola: links with Brazil. Journal of African Earth Sciences, 31, 383-402.

Claoué-Long, J.C., Compston, W., Roberts, J., Fanning, C.M., 1995. Two carboniferous ages: a comparison of SHRIMP zircon dating with conventional zircon ages and $^{40}Ar/^{39}Ar$ analysis. *Geochronology Time Scales and Global Stratigraphic Correlation*, SEPM Special Publication No 54, 1-21.

Cliff, R.A., Clemmey, H., 1976. Rb-Sr age of pegmatitic muscovite from Mindola Mine, Zambian Copperbelt. Ann. Rept. Res. Inst. Afr. Geol., Leeds Univ., 20, p. 68.

Clifford, T.N., Nicolaysen, L.O., Burger, A.J., 1962. Petrology and age of the Pre-Otavi Basement granite at Franzfontein, northern South-West Africa. Journal of Petrology, 3(2), 244-279.

Compston, W., Williams, I.S., Meyer, C., 1991. Initial Pb isotopic compositions of lunar granites as determined by ion microprobe. In: Taylor, H.P., Jr., O'Neill, J.R., Kaplan, I.R. (Eds.), *Stable Isotope Geochemistry: A tribute to Samuel Epstein*. The Geochemical Society Special Publication, 3, 473-486.

Cosi, M., de Bonis, A., Gosso, G., Hunziker, J., Martinotti, G., Moratto, S., Robert, J.P., Ruhlman, F., 1992. Late Proterozoic thrust tectonics, high-pressure metamorphism and uranium mineralization in the Domes area, Lufilian Arc, northwestern Zambia. Precambrian Research, 58, 215-240.

Daly, M.C., 1986. The intracratonic Irumide belt of Zambia and its bearing on collision orogeny during the Proterozoic of Africa. In: Coward, M.P., Ries, A. (Eds.), *Collisional Tectonics*. Geological Society of London, Special Publication, 19, 321-328.

Daly, M.C., 1988. Crustal shear zones in Central Africa: a kinematic approach to Proterozoic tectonics. Episodes, 11(1), 5-11.

Daly, M.C., Chakraborty, S.K., Kasolo, P., Musiwa, M., Mumba, P., Naidu, B., Namateba, C., Ngambi, O., Coward, M.P., (1984). The Lufilian arc and Irumide Belt of Zambia: results of a geotraverse across their intersection. J. Afr. Earth Sci., 2(4), 311-318.

Daly, M.C., Unrug, R., 1982. The Muva Supergroup of northern Zambia: a craton to mobile belt sedimentary sequence. Transactions of the Geological Society of South Africa, 85, 155-165.

Darnley, A.G., 1960. Petrology of some Rhodesian Copperbelt orebodies and associated rocks. Transactions of the Institution of Mining and Metallurgy, London, 69, 137-173; 371-398; 540-569.

Delhal, J., 1991. Situation géochronologique 1990 du Précambrien du Sud-Kasai et de l'Ouest-Shaba. Mus. Roy. Afr. Centr., Tervuren (Belg.); Dépt. Géol. Minéral., Rapp. Ann. 1989-1990, 119-125.

Delhal, J., Ledent, D., 1973. L'âge du complexe métasédimentaire de Luiza, region du Kasai (Zaïre). Ann. Soc. Géol. Belg., 94, 211-221.

Delhal, J., Ledent, D., Torquato, J.R., 1976. Nouvelles données géochronologiques reatives au complexe gabbro-noritique et charnockitique du bouclier du Kasaï et à son prolongement en Angola. Ann. Soc. Géol. Belg., 99, 211-226.

Demesmaeker, G., François, A., Oosterbosch, R., 1963. La tectonique des gisements cuprifères stratiformes du Katanga. In: Lombard, J., Nicolini, P. (Eds.), *Stratiform Copper Deposits in Africa, 2nd Part: Tectonics*. Assoc. Afr. Geol. Surveys, Paris, 47-115.

De Waele, B., Fitzsimons, I.C.W., 2004. The age and detrital fingerprint of the Muva Supergroup of Zambia: molassic deposition to the southwest of the Ubendian Belt. Geoscience Africa 2004, Abstract Volume 1, University of the Witwatersrand, Johannesburg, South Africa, 162-163.

De Waele, B., Wingate, M.T.D., Fitzsimons, I.C.W., Mapani, B.S.E., 2003. Untying the Kibaran knot: A reassessment of Mesoproterozoic correlations in southern Africa based on SHRIMP U-Pb data from the Irumide belt. Geology, 31(6), 509-512.

De Waele, B., Mapani, B 2002. Geology and correlation of the central Irumide Belt. Journal of African Earth Sciences, 35, 385-397.

Drysdall, A.R., Johnson, R.L., Moore, T.A., Thieme, J.G., 1972. Outline of the geology of Zambia. Geol. Mijnbouw, 51, 265-276.

Dürr, S.B., Dingledey, D.P., 1996. The Kaoko belt (Namibia): part of a late Neoproterozoic continental-scale strike-slip system. Geology, 24, 503-506.

Eberle, D., Hutchins, D.G., Rebbeck, R.J., Somerton, I., 1996. Compilation of the Namibian airborne magnetic surveys: procedures, problems and results. Journal of African Earth Sciences, 22, 191-205.

Feather, C.E., Willis, J.P., 1976. A simple method for background and matrix correction of spectral peaks in trace element determination by X-ray fluorescence spectrometry. *X-Ray Spectrometry*, **5**, 41-48.

Frets, D.C., 1969. Geology and structure of the Huab-Welwitschia area, South West Africa. Precambrian Research Unit, University of Cape Town, Bulletin, 5, 235 pp.

Garlick, W.G., 1961a. Structural evolution of the Copperbelt. In: Mendelsohn, F. (Ed.), *The Geology of the Northern Rhodesian Copperbelt*. Macdonald, London, 89-105.

Garlick, W.G., 1961b. Basement complex: Muva system. In: Mendelsohn, F. (Ed.), *The Geology of the Northern Rhodesian Copperbelt*. Macdonald, London, 21-30.

Garlick, W.G., Brummer, J.J., 1951. The age of the granites of the northern Rhodesia Copperbelt. Economic Geology, 46, 478-497.

Garrard, P., 1965. Chingola, Kalulushi and Ndola (Rural) Districts, Chingola Sheet. Annual Report for 1964, Geological Survey of Zambia, 2-3.

Garrard, P., 1996. The geology of the Chingola area: Explanation of Degree Sheet 1227, SE Quarter. Rep. Geol. Surv. Zambia, No. 66.

Goscombe, B., Hand, M., Gray, D., 2003. Structure of the Kaoko Belt, Namibia: progressive evolution of a classic transpressional orogen. J. Structural Geology, 25, 1049-1081.

Gray, A., 1929. An outline of the geology and ore deposits of the Nkana Concession. *15th International Geological Congress Guide Book (Excursion C22). Pretoria, South Africa*, 34-40.

Guj, P., 1970. The relationship between the “Franzfontein Granite” and the Huab and Khoabendus Formations northwest of Franzfontein, South West Africa. Annals of the Geological Survey of South Africa, 8, 45-51.

Gysin, M., 1933. Recherches géologiques et pétrographiques dans le Katanga méridional. Mémoir de l’Institut royale Coloniale belge, Sciences Naturelles et Médicales, 6(1), 259 pp.

Hanson, R.E., 2003. Proterozoic geochronology and tectonic evolution of southern Africa. In: Yoshida, M., Windley, B.F., Dasgupta, S. (Eds.), Proterozoic East Gondwana: Supercontinent Assembly and Breakup. Geological Society, London, Special Publications, 206, 427-463.

Hanson, R.E., Wardlaw, M.S., Wilson, T.J., Mwale, G., 1993. U-Pb zircon ages from the Hook granite massif and Mwembeshi dislocation: constraints on Pan African deformation, plutonism and transcurrent shearing in central Zambia. Precambrian Research, 63, 189-209.

Hanson, R.E., Wilson, T.J., Munyanyiwa, H., 1994. Geologic evolution of the Neoproterozoic Zambezi Orogenic Belt in Zambia. J. Afr. Earth Sci., 18, 135-150.

Hawkesworth, C.J., Kramers, J.D., Miller, R.McG., 1981. Old model Nd ages in Namibian Pan-African rocks. Nature, 289, 278-282.

Hawkesworth, C.J., Marlow, A.G., 1983. Isotope evolution of the Damara orogenic belt. In: Miller, R.McG. (Ed.), *Evolution of the Damara Orogen of South West Africa/Namibia*. Spec. Publ. Geol. Soc. S. Afr., Johannesburg, 11, 397-407.

Hoal, K.O., Hoal, B.G., Griffin, W.L., Armstrong, R.A., 2000. Characterization of the age and nature of the lithosphere in theTsumkwe region, Namibia. In: Miller, R.McG. (Ed.), *Special Issue: Henno Martin Commemorative Volume.* Communications Geological Survey Namibia, 12, 21-28.

Hoffman, K.-H., 1994. New constraints on the timing of continental breakup and collision in the Damara Belt. Conference on Proterozoic Crustal and Metallogenic Evolution, 29 August- 1 September, 1994, Windhoek, Namibia, p. 30.

Irvine, T.N., Baragar, W.R., 1971. A guide to the classification of the common volcanic rocks. Canadian Journal of Earth Sciences, 8, 527-548

Jackson, G.C.A., 1932. The geology of the N'changa district, Northern Rhodesia. Quarterly Journal of the Geological Society, London, 88, 443-515.

Jackson, M.P.A., Warin, O.N., Woad, G.M., Hudec, M.R., 2003. Neoproterozoic allochthonous salt tectonics during the Lufilian orogeny in the Katangan Copperbelt, central Africa. Geological Society of America Bulletin, 115(3), 315-330.

Jacob, R.E., Kröner, A., Burger, A.J., 1978. Areal extent and first U-Pb age of the pre-Damara Abbabis complex in the central Damara belt of South West Africa (Namibia). Geologische Rundschau, 67, 706-718.

Jacob, R.E., Moore, J.M., Armstrong, R.A., 2000. Zircon and titanite age determinations from igneous rocks in the Karibib District, Namibia: implications for Navachab vein-style gold mineralization. In: Miller, R. McG. (Ed.), Special Issue: Henno Martin Commemorative Volume. Communications Geological Survey Namibia, 12, 157-166.

Jedwab, J., 1997. Minéralogie des métaux du groupe du platine au Shaba, Zaïre. In: Charlet, J.M. (Ed.), 'Gisements stratiforme de cuivre et minéralisations associées'. Centenaire des premières études sur la géologie shabienne (Zaïre), Mém. Acad. Roy. Sci. d'Outre-Mer, Bruxelles, 325-355.

John, T., Schenk, V., Haase, K., Scherer, E. & Tembo, F., 2003. Evidence for a Neoproterozoic ocean in south central Africa from MORB-type geochemical signatures and P-T estimates of Zambian eclogites. Geology, 31, 243-246.

Kabengele, M., Lubala, R.T., Cabanis, B., 1991. Caractérisation pétrologique et géochimique du magmatisme ubendien du secteur de Pepa-Lubumba, sur le plateau de Marungu (Nord-Est du Shaba, Zaire). Signification géodynamique dans l'évolution de la chaîne ubendienne. Journal of African Earth Sciences, 13(2), 243-265.

Kabengele, M., Tshimanga, K., Lubala, R.T., Kapenda, D., Walraven, F., 1990. Geochronology of the calc-alkaline granitoids of the Marungu plateau (Eastern Zaïre - Central Africa). In: Rocci, G., Deschamps, M. (Eds.), New data in African Earth Sciences. Ext. abstr. 15th Coll. Afr. Geol., CIFEG Occ. Publ. 1990/22, Orléans, 51-55.

Kampunzu, A.B., Akanyang, P., Mapeo, R.B.M., Modie, B.N., Wendorff, M., 1998. Geochemistry and tectonic significance of the Mesoproterozoic Kgwebe metavolcanic rocks in northwest Botswana: implications for the evolution of the Kibaran Namaqua-Natal Belt. Geological Magazine, 135, 669-683.

Kampunzu, A.B., Rumvegeri, B.T., Kapenda, D., Lubala, R.T., Carn, J.-P.H., 1986. Les Kibarides d'Afrique centrale et orientale: une chaîne de collision. UNESCO, Geology for Economic Development, Newsletter/ Bulletin, 5, 127-137.

Key, R.M., Liyungu, A.K., Njamu, F.M., Somwe, V., Banda, J., Mosley, P.N., Armstrong, R.A., 2001. The Western arm of the Lufilian Arc in NW Zambia and its potential for copper mineralization. Journal of African Earth Sciences, 33, 503-528.

Key, R.M, Armstrong, R.A., 2000. Geology and geochronology of pre-Katangan igneous and meta-igneous rocks north of the Lufilian Arc in northwest Zambia. Journal of African Earth Sciences, 31, 36-37.

Klerkx, J., Liégeois, J.-P., Lavreau, J., Claessens, W., 1987. Crustal evolution of the Northeastern Kibaran belt, eastern and central Africa. In: Kröner, A. (Ed.), *Proterozoic Lithospheric Evolution*. American Geophysical Union, Geodynamics Series, 17, 217-233.

Klinck, B.A., 1977. The geology of the Kabompo Dome area. Explanation of Degree Sheet 1224, NE Quarter. Geological Survey Department, Zambia, Report No. 44, 27 pp.

Kokonyangi, J., Armstrong, R., Kampunzu, A.B., Yoshida, M., Okudaira, T., 2002. Magmatic evolution of the Kibarides Belt (Katanga, Congo) and implications for Rodinia reconstruction: field observations, U-Pb SHRIMP geochronology and geochemistry of granites. Extended Abstracts, 11th Quadrennial IAGOD Symposium and Geocongress 2002, 22-26 July 2002, Windhoek, Namibia, CD-ROM.

Kröner, A., Retief, E.A., Compston, W., Jacob, R.E., Burger, A.J., 1991. Single-grain and conventional zircon dating of remobilized basement gneisses in the central Damara belt of Namibia. South African Journal of Geology, 94(5/6), 379-387.

Kröner, S., Kröner, A., Konopasek, J.., Passchier, C., Hoffman, K.-H., 2002. Structure and geochronology of the Western Kaoko belt (NW Namibia). Abstract, 19th Colloquium of African Geology, El Jadida, Morocco, 19-22 March 2002, p. 112.

Lecompte, M., 1933. Le batholite de Mokambo (Katanga) et ses alentours. Mémoire de l'Institut Géologique, Université de Louvain, 7(3), 129-224.

Lefebvre,J.J., Cailteux,J., 1975. Volcanisme et minéralisations diagénétiques dans le gisement de l'Etoile, Shaba, Zaire. Ann. Soc. géol. Belg., 98, 89-107.

Legg, C., 1976. The geology and mineralisation of the Mkushi copper deposits. Ministry of mines and industry, Geological Survey Department, Zambia, Report No. 38.

Lenoir, J.L., Liégeois, J.-P., Theunissen, K., Klerkx, J., 1994. The Palaeo-proterozoic Ubendian shear belt in Tanzania: geochronology and structure. Journal of African Earth Sciences, 19, 169-184.

Liyungu, A.K., Njamu, F.J., 2000. The geology of the Lumwana West area. Explanation of Degree Sheet 1125, SW Quarter. Geological Survey Department, Zambia, Report No. 111, 44 pp.

Ludwig, K.R., 2000. Users Manual for Isoplot/Ex version 2.3, a geochronological toolkit for Microsoft Excel. Berkeley Geochronology Center, Special Publications, No. 1a.

Mapani, B.S., Rivers, T., Tembo, F., DeWaele, B, Katongo, C., 2004. Growth of the Irumide terranes and slices of Archaean age in eastern Zambia. Geoscience Africa 2004, Abstract Volume 2, University of the Witwatersrand, Johannesburg, South Africa, 414-415.

McCourt, S., Armstrong, R.A., Kampunzu, A.B., Mapeo, R.B.M., Morais, E., 2004. New U-Pb SHRIMP ages on zircons from the Lubango region, southwest Angola: insights into the Proterozoic evolution of south-western Africa. Geoscience Africa 2004, Abstract Volume 2, University of the Witwatersrand, Johannesburg, South Africa, 438-439.

Machairas, G., 1974. Découverte des roches volcano-detritiques associées à la minéralisation cuprocobaltifère du Shaba (Zaïre). C. R. Acad. Sci., Paris, 278, sér. D, 553-556.

Master, S., 1990. The "Ubendian" cycle in Equatorial and Southern Africa: Accretionary tectonics and continental growth. In: Rocci, G.,Deschamps, M. (Eds.), *New data in African Earth Sciences*. CIFEG Occ. Publ. 1990/22, Orléans, 41-44.

Master, S., 1993. Early Proterozoic assembly of "Ubendia" (Equatorial and Southern Africa and adjacent parts of South America): tectonic and metallogenic implications. In: Dia, A. (Ed.), *Symposium on the Early Proterozoic: Geochemical and Structural constraints, Metallogeny*. CIFEG Occ. Publ. 1993/23, Orléans (France), 103-107.

Master, S., Rainaud, C., Armstrong, R.A., Phillips, D., Robb, L.J., 2004. Provenance ages of the Neoproterozoic Katanga Supergroup (Central African Copperbelt), with implications for basin evolution. In: Robb, L.J., Sutton, S., Cailteux J. (Eds.), Special Issue on the Central African Copperbelt, Journal of African Earth Sciences.

Mayer, A., Sinigoi, S., Morais, E., 2000. The Kunene gabrro-anorthosite complex: coalescence of crystal mush intrusions during the early Kibaran. EOS, Transactions of the American Geophysical Union, 81, 1248-1249.

McMullan, S.R., Campbell, C.J., Koosimile, D.I., 1995. National gravity survey of Botswana- Second edition. In: Blenkinsop, T.G., Tromp, P.L. (Eds.), Sub-Saharan Economic Geology. Spec. Publ. Geol. Soc. Zimbabwe No. 3, A.A. Balkema, Rotterdam, 133-140.

Mendelsohn, F., 1961a. *The Geology of the Northern Rhodesian Copperbelt*. (Ed.) Macdonald, London, 523 pp.

Mendelsohn, F., 1961b. Basement Complex: Lufubu System. In: Mendelsohn, F. (Ed.), *The Geology of the Northern Rhodesian Copperbelt*. Macdonald, London, 18-19.

Mendelsohn, F., 1961c. Basement Complex: Granite. In: Mendelsohn, F. (Ed.), *The Geology of the Northern Rhodesian Copperbelt*. Macdonald, London, 19-21.

Miller, R. McG., 1983. Evolution of the Damara Orogen of South West Africa/Namibia. In: Miller, R.McG. (Ed.), *Evolution of the Damara Orogen of South West Africa/Namibia*. Geological Society of South Africa, Special Publications, 11, 431-515.

Money, N.J., 1972. An outline of the geology of Western Zambia. Geological Survey of Zambia, Records, 12, 103-123.

Morais, E., Sinigoi, S., Mayer, A., Miguel, L.G., 2000. The Kunene Complex: Emplacement of a composite, massive anorthosite body within a Kibaran extensional context. GeoLuanda 2000 International

Conference, Guidebook Post-Conference Field Excursion Lubango-Kunene, 25-28 May 2000, 11 pp.

Ng'ambi, O., Boelrijk, N.A.I.M., Priem, H.N.A., 1986. Geochronology of the Mkushi gneiss complex, Central Zambia. Precambrian Research, 32, 279-295.

Ngoyi, K., Liégeois, J.-P., Demaiffe, D., Dumont, P., 1991. Age tardi-ubendien (Protérozoïque inférieur) des dômes granitiques de l'arc cuprifère zaïro-zambien. C. R. Acad. Sci., Paris, 313, Sér. II, 83-89.

Norrish, K., Hutton, J.T., 1969. An accurate X-ray spectrographic method for the analysis of a wide range of geological samples. Geochim. Cosmochim. Acta 33(4), 431-453.

Omenetto, P., 1973. Mineralizzazioni cuprifere e granitizzazione: alcune osservazioni sul Distretto di Mkushi (Zambia). Resoconti dell'Associazione Mineraria Sarda, Cagliari, 78(6), 1-9.

Omenetto, P., 1974. Minéralisations à cuivre et granitisation: le District de Mkushi (Zambie). Proc. 7th Colloquium on African Geology, Florence, 25-27 April 1973, Istituto di Mineralogia e Petrologia dell'Universita di Padova, Padua, Italy, 6 pp.

Pienaar, P.J., 1961. Basement complex: Mineralization in the Basement. In: Mendelsohn, F. (Ed.) The Geology of the Northern Rhodesian Copperbelt. Macdonald, London, 30-41.

Pinna, P., Cocherie, A., Thieblemont, D., Feybesse, J.-L., Lagny, P., 1996. Évolution géodynamique du Craton Est-Africain et déterminisme gîtologique. Chronique de Recherche Minière, No. 525, 33-43.

Pinna, P., Cocherie, A., Thieblemont, D., Jezequell, P., Kayagoma, E., 1999. The Archaean evolution of the Tanzanian Craton (2.93-2.53 Ga). Journal of African Earth Sciences, 28(4A), 62-63.

Porada, H., 1974. The Khoabendus Group in the area northwest of Kamanjab and in the southeastern Kaokoveld, South West Africa. Bulletin of the Geological Survey of South Africa, No. 4, South West Africa series, 23 pp.

Porada, H., Berhorst, V., 2000. Towards a new understanding of the Neoproterozoic-Early Palaeozoic Lufilian and northern Zambezi belts in Zambia and the Democratic Republic of Congo. J. Afr. Earth Sci., 30, 727-771.

Prave, A.R., 1996. Tale of three cratons: Tectonostratigraphic anatomy of the Damara orogen in northwestern Namibia and the assembly of Gondwana. Geology, 24(12), 1115-1118.

Rainaud, C., Master, S., Armstrong, R.A. and Robb, L.J., 2003. A cryptic Mesoarchaean terrane in the basement to the Central African Copperbelt. Journal of the Geological Society, London, 160, 11-14.

Rainaud, C., Master, S., Armstrong, R.A., Phillips, D., Robb, L.J., 2004. Monazite U-Pb dating and $^{40}Ar/^{39}Ar$ thermochronology of metamorphic events during the Lufilian orogeny, Central African Copperbelt. In: Robb, L.J., Sutton, S., Cailteux J. (Eds.), Special Issue on the Central African Copperbelt, Journal of African Earth Sciences.

Reeves, C.V., 1978. The Gravity Survey of Ngamiland 1970-71. Botswana Geological Survey Department, Bulletin 11, 84 pp.

Reeves, C.V., 1979. The reconnaissance aeromagnetic survey of Botswana-II: Its contribution to the geology of the Kalahari. In: McEwan, G. (Ed.), The proceedings of a seminar on geophysics and the exploration of the Kalahari. Botswana Geological Survey Department, Bulletin 22, 67-92.

Ring, U., Kröner, A., Toulkerides, T., 1997. Palaeoproterozoic granulite facies metamorphism and granitoid intrusions in the Ubendian-Usagaran Orogen of northern Malawi, east-central Africa. Precambrian Research, 85, 27-51.

Robert, M., 1956. *Géologie et géographie du Katanga y compris l'étude des ressources et de la mise en valeur*. Hayez, Bruxelles, 620 pp.

Rumvegeri, B.T., 1989. Le Précambrien de l'ouest du Lac Kivu (Zaïre) et sa place dans l'évolution géodynamique de l'Afrique centrale et orientale. Pétrologie et tectonique. IGCP Project No. 255, Metallogeny of the Kibara Belt, Central Africa, Bulletin-Newsletter 2, TU Braunschweig, MRAC Tervuren, 73-76.

Rumvegeri, B.T., 1991. Tectonic significance of Kibaran structures in Central and Eastern Africa. Journal of African Earth Sciences, 30, 629-639.

Saviaro, K., 1978. Airborne magnetic and gravity surveys in Zambia. Geological Survey Department, Zambia, Occasional Paper No. 96, 13 pp.

Saviaro, K., 1979. Preliminary analysis of the airborne magnetic surveys in Zambia. In: McEwan, G. (Ed.), The proceedings of a seminar on geophysics and the exploration of the Kalahari. Botswana Geological Survey Department, Bulletin 22, 159-183.

Schandelmeier, H., 1981. The Precambrian of NE-Zambia in relation to the dated Kate, Mambwe and Luchewe intrusives. Geologische Rundschau, 70, 956-971.

Schandelmeier, H., 1983. The geochronology of post-Ubendian granitoids and dolerites from the Mambwe area. Northern Province, Zambia. Report Institute of Geological Sciences, 83/1, 40-46.

Schenk, V., Appel, P., 2001. Anti-clockwise P-T path during ultrahigh-temperature (UHT) metamorphism at ca. 1050 Ma in the Irumide belt of eastern Zambia. Berichte der Deutschen Mineralogischen Gesellschaft, Beihefte zum European Journal of Mineralogy, 13, p. 161.

Schenk, V., Appel, P., 2002. UHT-metamorphism in the Irumide Belt of Zambia: An anti-clockwise *P-T* path and a concordant monazite age at 1.05 Ga. Abstract, 19th Colloquium of African Geology, El Jadida, Morocco, 19-22 March 2002, p. 165.

Seth, B., Armstrong, R.A., Brandt, S., Villa, I.M., Kramers, J.D., 2003. Meso-proterozoic U-Pb and Pb-Pb ages of granulites in NW Namibia: reconstructing a complete orogenic cycle. Precambrian Research, 126, 147-168.

Seth, B., Kleinhanns, I.C., Kramers, J.D., Armstrong, R.A., 2001. Crustal de-coupling of Hf and Nd isotope systems in high-grade metamorphic rocks. AGU Fall Meeting, EOS, Transactions of the American Geophysical Union, 82, V22B-1030.

Seth, B., Kröner, A., Mezger, K., Nemchin, A.A., Pidgeon, R.T., Okrusch, M., 1998. Archaean to Neoproterozoic magmatic events in the Kaoko belt of NW Namibia and their geodynamic significance. Precambrian Research, 92, 341-363.

Singletary, S.J., Hanson, R.E., Martin, M.W., Crowley, J.L., Bowring, S.A., Key, R.M., Ramokate, L.V., Direng, B.B., Krol, M.A. (2003). Geochronology of basement rocks in the Kalahari Desert, Botswana, and implications for regional Proterozoic tectonics. Precambrian Research, 121, 47-71.

Snelling, N.J., Hamilton, E.I., Drysdall, A.R., Stillman, C.J., 1964. A review of age determinations from Northern Rhodesia. Economic Geology, 59, 961-981.

Steven, N., Armstrong, R., 2003. A metamorphosed Proterozoic carbonaceous shale-hosted Co-Ni-Cu deposit at Kalumbila, Kabompo Dome: The Copperbelt Ore Shale in northwestern Zambia. Economic Geology, 98, 893-909.

Steven, N., Armstrong, R., Smalley, T., Moore, J., 2000. First geological description of a Late Proterozoic (Kibaran) metabasaltic andesite-hosted chalcocite deposit at Omitiomire, Namibia. In: Clauer, J.K., Price, J.G., Struhsacker, E.M., Hardyman, R.F., Morris, C.L. (Eds.), *Geology and Ore Deposits 2000: The Great Basin and Beyond: Symposium Proceedings*. Geological Society of Nevada, Reno, Nevada, 2, 711-734.

Stillman, C.J., 1965. The geology of the Musofu river and Mkushi areas: explanation of degree sheet 1329, part of NW quarter, and SW quarter. Geological Survey Department, Zambia, Report No. 12, 52 pp.

Tack, L., Liégeois, J.-P., Deblond, A., Duchesne, J.C., 1994. Kibaran A-type granitoids and mafic rocks generated by two mantle sources in a late orogenic setting (Burundi). Precambrian Research, 68, 323-356.

Tack, L., Fernandez-Alonso, M., Wingate, M., Deblond, A., 1999. Critical assessment of recent unpublished data supporting a single and united geodynamic evolution of the Sao Francisco-Congo-Tanzania cratonic blocks in the Rodinia configuration. Journal of African Earth Sciences, 28(4A), 75-76.

Tack, L., Williams, I., Bowden, P., 2002. SHRIMP constraints on early post-collisional granitoids of the Ida Dome, Central Damara (Pan-African) Belt, western Namibia. Extended Abstracts, 11th Quadrennial IAGOD Symposium and Geocongress 2002, 22-26 July 2002, Windhoek, Namibia, CD-ROM.

Tegtmeyer, A., Kröner, A., 1985. U-Pb zircon ages for granitoid gneisses in northern Namibia and their significance for Proterozoic crustal evolution of Southern Africa. Precambrian Research, 28, 311-326.

Tembo, F., de Waele, B., Nkemba, S., 2002. Syn- to post-orogenic granitoid magmatism in the Irumide belt of Zambia: geochemical evidence. Africa Geoscience Review, 9(1), 1-17.

Tera, F., Wasserburg, G.J., 1972. U-Th-Pb systematics in three Apollo 14 basalts and the problem of initial Pb in lunar rocks. Earth and Planetary Science Letters, 14, 281-304.

Theunissen, K., Lenoir, J.-L., Liégeois, J.-P., Delvaux, D., Mruma, A., 1992. Major Pan-African imprint in the Ubendian belt of SW Tanzania: U-Pb on zircon geochronology and structural context. C. R. Acad. Sci. Paris, 314, Sér. II, 1355-1362.

Thieme, J.G. (1970). The Geology of the Mansa Area. Explanation of Degree Sheet 1128, parts of NW Quarter and NE Quarter. Geological Survey of Zambia, Report No. 26.

Thieme, J.G., 1971. The Geology of the Musonda Falls Area. Explanation of Sheet 1028, SE Quarter. Geological Survey of Zambia, Report No. 32, 25 pp.

Thieme, F., Johnson, R.L., 1981. 1:1,000,000 Geological Map of Zambia. Zambia Geological Survey Department, Lusaka.

Truter, F.C., 1935. The geology and petrography of the Mkushi-Lunsemfwa area, Northern Rhodesia. Unpublished thesis, University of Cape Town.

Tshimanga, K., Lubala, T., 1990. Evolution géodynamique de la chaîne ubendienne (Protérozoïque Inférieur) de l'Afrique centrale et orientale: Nouvelles données et mise au point. In: Rocci,G., Deschamps, M. (Eds.), *Recent data in African Earth Sciences*. Ext. abstr. 15th Coll. Afr. Geol., CIFEG Occ. Publ. 1990/22, Orléans, 45-49.

Wakefield, J., 1978. Samba: a deformed porphyry-type copper deposit in the basement of the Zambian Copperbelt. Institution of Mining and Metallurgy, 87, B43-B52.

Wendorff, M., 2003. Stratigraphy of the Fungurume Group- evolving foreland basin succession in the Lufilian fold-thrust belt, Neoproterozoic-Lower Palaeozoic, Democratic Republic of Congo. South African Journal of Geology, 106, 47-64.

Winchester, J.A., Floyd, P.A., 1977. Geochemical discrimination of different magma series and their differentiation products using immobile trace elements. Chemical Geology, 20, 325-343.